



**HAL**  
open science

## **Influence of kerosene flame on fire-behaviour and mechanical properties of hybrid Carbon Glass fibers reinforced PEEK composite laminates**

Benoît Vieille, Alexis Coppalle, E. Schuhler, A. Chaudhary, Adem Alia, N. Delpouve, Aurélie Bourdet

### ► To cite this version:

Benoît Vieille, Alexis Coppalle, E. Schuhler, A. Chaudhary, Adem Alia, et al.. Influence of kerosene flame on fire-behaviour and mechanical properties of hybrid Carbon Glass fibers reinforced PEEK composite laminates. *Composite Structures*, 2022, 279, pp.114786. 10.1016/j.compstruct.2021.114786 . hal-04355471

**HAL Id: hal-04355471**

**<https://normandie-univ.hal.science/hal-04355471v1>**

Submitted on 22 Jul 2024

**HAL** is a multi-disciplinary open access archive for the deposit and dissemination of scientific research documents, whether they are published or not. The documents may come from teaching and research institutions in France or abroad, or from public or private research centers.

L'archive ouverte pluridisciplinaire **HAL**, est destinée au dépôt et à la diffusion de documents scientifiques de niveau recherche, publiés ou non, émanant des établissements d'enseignement et de recherche français ou étrangers, des laboratoires publics ou privés.



Distributed under a Creative Commons Attribution - NonCommercial 4.0 International License

## **Influence of kerosene flame on fire-behaviour and mechanical properties of hybrid Carbon Glass fibers reinforced PEEK composite laminates**

Vieille B.<sup>1</sup>, Coppalle A.<sup>2</sup>, Schuhler E.<sup>2</sup>, Chaudhary A.<sup>2</sup>, Alia A.<sup>1</sup>, Delpouve N.<sup>1</sup>, Bourdet A.<sup>1</sup>

<sup>1</sup> Normandie Univ, UNIROUEN Normandie, INSA Rouen, CNRS, Groupe de Physique des Matériaux  
76800 St Etienne du Rouvray

<sup>2</sup> Normandie Univ, UNIROUEN Normandie, INSA Rouen, CNRS, CORIA, 76800 St Etienne du  
Rouvray

### **Abstract**

This work examines the influence of kerosene flame exposure on the residual mechanical behavior (tension and compression) of hybrid quasi-isotropic composite laminates consisting of carbon/glass fibers and a PEEK thermoplastic matrix. The influence of a kerosene flame exposure (116 kW/m<sup>2</sup> and 1100 °C), on the composites structural integrity was examined as a function of exposure time (5-10-15 min). The changes in the tensile and compressive properties (axial stiffness and strength) were compared with respect to the virgin materials (experiencing no prior flame exposure). The discussions on fire- and mechanically-induced damage mechanisms are supported by fractographic analysis of specimens. It is therefore possible to better understand how the fire-induced damages within the laminates micro- and meso-structures modify the mechanical behavior of flame-exposed laminates. Regardless the exposure time, the kerosene flame exposure involves in-plane and through-thickness temperature gradients, which ultimately create two well defined areas within the laminates: an extensively delaminated one (the one close to the exposed surface) and a relatively well preserved one (close to the back surface). From the present work, it is possible to conclude that the mechanical properties in tension are severely affected (-50% in stiffness and -70% in strength) by prolonged exposures to kerosene flame (15 min) with respect to as-received specimens. When compared to the 5 min case, flame exposure time (ranging from 5 to 15 min) seems to have little very influence on tensile properties and the effect is moderate on compressive properties. The barrier formed by an extensive thermally-induced delamination contributes to relatively preserve the structural integrity of the plies close to the back surface. The mechanical loading is taken up by the 0° fibers in non-delaminated areas of the specimens, resulting in preserving the residual mechanical in tension and in compression.

**Keywords:** thermoplastic; carbon fibers; kerosene flame; thermal analysis; mechanical testing



## **1. Introduction**

While there is increasing demand for Polymer-Matrix Composites (PMCs) in aeronautical applications, their use is limited by their structural susceptibility to fire conditions. Thermosetting (TS) polymers have been the mainstays of aerospace composites since their introduction to aircraft [1]. Over the past thirty years, thermoplastics (TP) based composites represent a promising alternative in aeronautics. The recent development of TPs with improved temperature and solvent resistance fosters the interest for applications in several engineering fields, where they are considered as matrices in high-performance composites [2-3]. They are characterized by a few attractive properties such as repeatable processing and recyclability, excellent impact toughness and low water uptake. These qualities make TP polymers attractive as a matrix in fibers reinforced PMCs. The main drawback of high-performance thermoplastics (like PEEK, PEKK and PPS) concerns their process ability, which is more difficult than the one of thermosetting composite systems [4]. Significant efforts have been devoted to developing melt-processable solutions and high compatibility with carbon fibers [5-6]. However, high-temperature resistance and impact toughness are the two most important technical requirements for practical applications of thermoplastic composites especially in aerospace [3][7]. The recent air disasters have revealed that the issue of fire is at the heart of the concerns of the aeronautics industry. The use of polymer matrix composite materials in aeronautic applications is today confronted with ever more demanding safety standards to which it is imperative to provide reliable and measurable answers [8-15]. Therefore, it is essential to enable manufacturers to understand/predict the thermomechanical response of composite materials in different configurations of use and, ultimately, of their parts and assemblies. The demand for experimental characterization means representative of critical conditions in service is therefore strong from industrialists who have identified a technological barrier in the fire resistance of polymer matrix composite materials [16]. When composites are exposed to high temperatures, the organic matrices start to decompose with the release of heat, toxic volatile and smoke. Therefore, it is very important to understand the structural properties of TP-based composites under fire and to assess their residual mechanical properties. Thus, the changes in both physicochemical and mechanical behaviors due to the interaction of fire on TP-based composites still need investigations.

### **1.1 Polymer Matrix Composites (PMCs) under fire conditions**

Aircraft-powerplant certification guidelines require large-scale fire tests to assess the ability of materials to act as firewalls. In their work, Chavez et al. developed a small-scale screening method [19]. Bare and protected carbon/epoxy specimens were exposed to an 1100 °C flame for 15 min, in accordance with service conditions met in aviation regulations. Thus, in order to test the fire resistance of PMCs, several standard tests specific to aeronautical applications are commonly used [20]. In particular, two different types of burner are described in the international standards for civil aircraft

fire resistance [19-20], one type of burner using propane as fuel [15] and the other type using kerosene [21]. Chazelle et al. have compared the degradation induced by kerosene and propane flames providing the same heat flux (110 kW/m<sup>2</sup>). They concluded that the mass loss rate is slower with the kerosene flame [22]. The maximum temperature value at the back surface is lower (about 150 °C) compared to the value obtained with a propane flame. A high amount of soots is observed in the laminates exposed to a kerosene flame. It results in the formation of a char layer on the exposed surface, which may contribute to reduce the heat transfer between the impinging flame and the specimen surface. Similarly, Le Neve et al. have pointed out differences on the qualification results depending on the burner type [23]. Even though flame exposure presents multiple advantages, so far, most of the laboratory scale studies are performed with a cone calorimeter to apply a radiative heat flux on the sample [24]. However, a direct flame impact is a more realistic thermal stress [25-27] and heat flux greater than 100 kW/m<sup>2</sup> can be easily reached for many fire scenarios [28]. The literature dealing with the fire response of TS-based composites is very rich [16]. But there are fewer references dealing with TP composites. Most of the results available in the literature on the fire behavior of TP-based materials have been obtained from cone calorimeter thermal aggression [1-7][28], of a propane burner on polyphenylene sulfide composites [15], or of a kerosene burner on PolyEther–Ketone–Ketone (PEKK) composites [26-27]. Thermal degradation analysis based on TGA tests under inert and oxidative conditions have been conducted by Tadini et al. [29], then Grange et al. [30-33]. They concluded that PEKK-based composites have a higher thermal performance than phenolic-based composites. A NexGen burner designed by the Federal Aviation Administration (FAA) was used to get a standardised flame intended to be a realistic scenario of an in-service or post-impact fire event. Such device allows the investigations of the burn-through resistance and the thermal behaviour of C/PEKK laminates [26-27]. These references only focused on the thermal degradation but no significant attention was paid to the residual mechanical properties. Most studies on that subject only refer to the influence of a prior thermal loading (by means of a cone calorimeter) on the residual mechanical behaviour (either in tension or compression), as pointed out in the next section.

## **1.2 Post-fire residual mechanical properties**

With respect to TS-based composites, the reason for the superior residual properties of TP-based composites is not fully understood [16]. It is assumed that TP composites generally have higher decomposition temperatures, yield high amounts of char, and are less susceptible to delamination cracking than TS laminates [8][10]. Char formation is expected to influence the residual properties of laminates, as it is known to retain the structural integrity of a fire-damaged composite by holding the fibers in place after the polymer matrix has been degraded [34-40]. In addition, melting and resolidification of the thermoplastic matrix positively affect the post-fire properties by maintaining the cohesion of the fibers network [9]. As a result, the analysis of the post fire tensile properties shows that prior severe fire exposures (medium to high heat flux – long exposure time) are more detrimental

to C/Epoxy than to C/PPS laminates. At last, most references dealing with the post-fire mechanical properties of TP-based composites are focused on the influence of cone calorimeter heat fluxes (ranging from 20 to 60 kW/m<sup>2</sup>). However, there are very few studies dealing with the influence of a kerosene flame exposure on the residual mechanical properties of PMCs [41]. While studying the tensile behaviour of quasi-isotropic carbon/epoxy laminates exposed to an 1100 °C methane flame and quenched at different intervals, Chavez et al. observed that the Ultimate Tensile Strength (UTS) reaches a plateau where loads could not be transferred between axial and transversal fibers due to matrix absence [19]. Thus, the residual UTS is solely attributed to the axially oriented fibers (0°) that bore the load until rupture. They also assessed the effectiveness of protective candidate materials by comparing the temperature distribution on the back surface and the UTS. Their results show good correlation between temperature reduction and residual strength enhancement. In a study dealing with E-glass/vinyl ester (VE) laminates and E-glass/VE balsa core sandwich composites, Ulven et al. have observed the development of char through the thickness of the materials resulting from the decomposition of the polymer matrix [42]. The residual char is very porous, brittle, and that is detrimental to the structural integrity of the composite parts. Low velocity impact response of PMCs was found to decrease after fire exposure (80 kW/m<sup>2</sup>, 800 °C) even for short periods of time (i.e. <100 s). Ultimately, very little work has been done in the literature to investigate the post-fire residual mechanical behaviour of TP-based composite materials. This is what motivated the present study.

### **1.3 Objectives of the work**

The present work was aimed at investigating the influence of the kerosene flame exposure time (5-10-15 min) on the fire behavior and the residual mechanical behaviour (tensile and compressive) of hybrid Carbon Glass fibers reinforced PEEK composite laminates (CG/PEEK) composite laminates. These investigations are intended to examine the effect of thermal degradation due to flame exposure on the composites structural integrity by comparing the changes of the mechanical properties (axial stiffness and strength) with respect to the virgin materials. The discussions on fire- and mechanically-induced damage mechanisms are supported by fractographic analysis of specimens. It is therefore possible to better understand how the fire-induced damages within the laminates micro- and meso-structures modify the mechanical behavior of flame-exposed laminates.

## **2. Materials and specimens**

The laminates used in this study are obtained by thermo-compression. They consist of a PEEK thermoplastic matrix reinforced with a continuous carbon fiber fabric (Tenax®-E HTA40 3K), structured in a 5-harness satin weave. 16 plies laminates with a quasi-isotropic lay-up [(0/90)<sub>V</sub>, (0/90), (±45), (0/90), (±45), (0/90), (±45), (0/90)]<sub>S</sub> have been considered in the present work. They have two outer plies of glass fabric (5-harness satin weave) and PEEK matrix noted as CG/PEEK, the 0.08 mm thick (0/90)<sub>G</sub> surface glass fabric is used as corrosion protection and electrical

protection with the aim of reducing the galvanic torque and thus avoiding galvanic corrosion of aluminum and steel with carbon. The main mechanical properties of the elementary ply are specified in Tab. 2. The laminates average thickness is about 4.5 mm. Tensile specimens have dog-bone geometry [8-10], whereas compressive specimens are rectangular plates whose dimensions are 150x100 mm<sup>2</sup> [13][43-44] cut by water jet from 600x600 mm<sup>2</sup> plates. Three samples have been tested in the following configurations:

- As received (referred to as virgin state),
- After a 5 min exposure to a kerosen flame
- After a 10 min exposure to a kerosen flame
- After a 15 min exposure to a kerosen flame

### **3. Experimental set-up**

#### **3.1 Kerosene burner bench**

The burner shown in figure 1 is made with a domestic device (Cuenod manufacturer). The kerosene is injected in a nozzle generating a hollow cone spray with an angle equal to 80° and a maximum flow rate of 0.3 g/s. This flow rate is controlled with a mass flow meter (MINI CORI-FLOW™, Bronkhorst), and it can be adjusted. Airflow is also controlled with a mass flow meter (EL-FLOW® Prestige, Bronkhorst).

The air to fuel ratio has been selected at 0.85 of the stoichiometric value, in order to obtain heat flux and temperatures values close to the standard values (116 kW/m<sup>2</sup> and 1100 °C) at the sample location. The flame at the exit of the turbulator is a wide and turbulent jet. Therefore, a 50 mm diameter steel tube is installed after the turbulator to channel the hot combustion gases on the exposed area of the sample. Details of the experimental set-up are presented in figure 1. With this design, an efficient mixing occurs inside the first part of the flame tube, and in its remaining part, the flow turbulence is strongly damped. At the flame tube exit, no kerosene droplets are observed and the combustion is completed. Thus, the thermal stress on the sample is due to the hot gas mixture of the combustion products [45-46]. The flame tube diameter is chosen equal to the diameter of the sample exposed surface.

The composite samples described in section 2 are placed on a dedicated sample holder for the test. The sample holder is presented in figure 2. The composite sample is placed between two insulation layers and the assembly is clamped by two steel plates. On both sides of the sample holder, an 80 mm side square aperture is made. On the front side, the sample is facing the burner output. On the backside, the temperature measurement is performed. This sample holder has two major aims. The first one is to prevent the surrounding of the sample by the flame. The second one is to maintain the integrity of the sample border. This is of great interest to perform post-fire mechanical tests. The 80 mm square

aperture is chosen in order to maintain a uniform heat flux on the exposed sample surface while maintaining at least 50 mm on the sample border.

### **3.2 Thermal and physico-chemical analysis**

Thermogravimetric analysis tests were conducted in a nitrogen atmosphere using a TA Discovery device. Measurements were performed on samples of about 5 mg with N<sub>2</sub> flow rate of 25 ml/min from 50 °C to 900 °C. Different heating rates were considered from 10 to 500 °C/min. To improve the accuracy of the measurement, particularly at high rates, the calibration procedure included a baseline, a calibration in temperature (Curie point of nickel) and a calibration in mass (reference masses) and mass loss (calcium oxalate).

### **3.3 Mechanical testing**

After kerosene-flame exposure, monotonic tensile and compressive tests were performed using a 100kN capacity load cell of a MTS 810 servo-hydraulic testing machine in displacement-controlled mode at Room Temperature (RT). The tensile mechanical properties were determined according to the European standards EN 6035 [47]. In agreement with the requirements of the Airbus Industries Test Method (AITM 1-0010), the specimen is stabilized by a 90×130 mm<sup>2</sup> frame consisting of anti-buckling knife-edges and clamping blocks as shown on Figure 3 [48].

### **3.4 Digital Image Correlation (DIC) technique**

A two-dimension DIC technique was used during compressive loading to investigate the onset of macroscopic buckling bands [13]. A DIC pattern is painted on the specimen surface with a non-periodic texture and without preferred orientation. The use of DIC technique at high temperature requires the use of a high intensity source combined with a fiber optic light guide that is used to illuminate the patterns on the surface of the specimen placed into the thermal chamber. A

Grasshopper® high-speed monochrome camera allows digital images to be recorded at full resolution (1920×1200 pixels), and at a rate of one frame-per-second during thermomechanical loading.

Ultimately, the Green-Lagrange strain field is derived from the 2D displacement field by means of the VIC-2D correlation software (provided by Correlated Solutions Company).

### **3.5 Fractographic analysis**

Microscopic observations have been carried out by means of a numerical optical microscope Keyence VHX-5000 to build 3D pictures of damaged areas. Fractographic analysis was conducted on samples after kerosene flame exposure as well as after mechanical loading.

## 4. Results and discussion

### 4.1 TGA results

Before investigating the influence of kerosene flame exposure on the degradation of laminates micro- and meso-structure, it seems relevant to consider first the influence of different heating rates on the thermal decomposition of CG/PEEK laminates under a nitrogen atmosphere (Figure 4). The purpose was here to consider values of heating rates close to the ones encountered during flame exposure, i.e., about 600 K/min and to compare the results with those obtained from measurement at conventional rates. Thus, TGA experiments were performed at rates ranging from 10 to 500 K/min. According to Figure 4a, the thermal decomposition of CG/PEEK laminates exhibits, independently on the heating rate, a single step of degradation that was interpreted as the result of random chain scission [16].

For all samples, the thermal decomposition starts at a temperature higher than the processing temperature of PEEK (350 °C). The thermal degradation of PEEK begins around 550 °C and the maximum degradation rate is recorded above 600 °C. From this result, we can confirm that the PEEK is thermally stable up to 450 — 500 °C at least, and therefore it is a suitable material for high-temperature applications. On the other hand, we observe that the heating rate influences both the onset of degradation  $T_{onset}$ , defined there as the temperature for which the sample mass is equal to 95% of its initial mass, and the residual mass at 700 °C, consecutive to the one-step degradation (Figure 4b). When the heating rate increases from 10 to 200 K/min,  $T_{onset}$  increases accordingly from 583 to 627 °C, that being the expected dependence of characteristic degradation temperatures on the rate of analysis. However, when increasing the rate from 200 to 500 K/min,  $T_{onset}$  starts decreasing from 627 to 610 °C. Such a profile can be explained in terms of thermal lags, as reported and discussed for calorimetric measurement at similar rates [49]. Those lags exist between the cell and the furnace, the instrument and the sample, and even within the sample, fairly highlighting the kind of temperature gradient the material is subjected during a flame aggression. The possibility that different degradation mechanisms will occur at high heating rates is not excluded either, as the residual mass intriguingly decreases from 82 to 77% when increasing the heating rate from 10 to 500 K/min. Indeed, although authors accord themselves in the literature around the thermal decomposition of the PEEK matrix essentially proceeding by chain scission, this breaking operates randomly, i.e., on various chemical groups, which is expected to generate different intermediates and decomposition products [50], that will influence the resulting material properties. Besides, temperature gradients are more likely to be

observed at high rates, thus leading to structural changes at the mesoscale. To investigate these modifications, the kerosene flame behavior is investigated in the subsequent section.

#### **4.2 Kerosene flame behaviour**

When subjected to combined thermal and mechanical loadings, the structural response of PMCs near or above the pyrolysis temperature is difficult to investigate as it is difficult to dissociate the influence of thermally and mechanically induced damages on the structural capabilities of the laminates [12-13].

Considering the results of thermal analysis presented in the previous section, the influence of exposure time on CG/PEEK laminates exposed to kerosene flame is investigated. When they are subjected to elevated temperatures, PMCs typically experience significant degradation of the polymer matrix resulting in reduced transverse and interlaminar shear strength and stiffness [34]. PMCs also have much lower thermal conductivities than metals, which create larger temperature gradients within the laminates. These temperature gradients lead to significant thermal stresses and degradation gradient in the polymer matrix resulting in heterogeneous damage modes. The type and the severity of damages depend on the degree and distribution of thermal degradation as well as the loading conditions (tension or compression, stress concentration).

Under one-side kerosene flame exposure, the exposed surface is severely degraded whereas the back surface only experiences little PEEK matrix melting (Fig. 5). This testing configuration is of particular interest as localized thermal loading (and subsequent degradation) is more likely to happen in an actual fire event such as compartment fire where damage will occur locally to adjacent structures [34]. In the center of the specimen, thermally induced degradation is the most severe. Carbonaceous char has formed along with the PEEK matrix pyrolysis. Pyrolysis is completed on the exposed surface as revealed by the observation of the glass fibers. It is worth noting that the degradation of the exposed surface is limited due to the protection action of the sample holder (an 80x80 mm<sup>2</sup> windows) that prevents the flame from directly degrading it (Fig. 2). The magnitude of temperature and thermally-induced degradation gradients significantly depends on the exposure time. As expected, the degraded area becomes larger as the exposure times increases on the exposed and back surfaces. The same remark can be made when observing the damages within the laminates through-thickness (Fig. 6). It clearly appears that the extensively delaminated area, resulting from the PEEK matrix pyrolysis initiated on the exposed surface, has reached half of the laminates thickness after 5- and 10-minutes flame exposure. After a 15 min exposure, the damaged area has reached about 2/3 of the laminates thickness. When subjected to fire conditions, the fast temperature increase resulting to the thermal expansion of matrix polymer and thermal contraction of the carbon fibre [51] leads to fibre-matrix

debonding and delamination that usually acts as barriers for heat conduction [52]. Depending on the intensity of thermal aggression and the testing environment (oxidative or non-oxidative), PMCs may also experience pyrolysis and the subsequent removal of the constitutive materials due to thermo-chemical ablation [34]. The barrier formed by extensive delamination contributes to involve the separation of the laminates in two well-defined areas: an extensively delaminated one and a relatively well preserved one. Both laminates areas are separated by a perfect delamination, as shown by the large space between the upper and lower parts. These damage mechanisms can be discussed along with the TGA tests conducted at different heating rates. Indeed, we reported that the heating rate influences the residual mass of the material, which suggests that the material undergo more severe structural damages. Obviously, the temperature gradient within the sample increases with the heating rate. Therefore, structural heterogeneity is evidenced at the meso scale. The material is divided into two areas, a degraded and a preserved one. The higher mass loss, recorded from TGA at high heating rates, can thus be interpreted as the consequence of severe localized degradation, as revealed by through-thickness macroscopic observations. As previously discussed, it might also be the consequence of differences between chain scissions occurring at the molecular scale. Obviously, these thermally induced damages are expected to significantly influence the residual mechanical behavior and properties in tension and in compression. More specifically, the structural capabilities (stiffness and strength) of the damage areas should be affected.

### **4.3 Residual mechanical behaviour**

Localized fire exposure occurs when the composite laminates is subjected to a constant intensity thermal loading on the laminates exposed face [34]. This type of loading leads to through-thickness and in-plane temperature gradients in the laminates. As was pointed previously, these temperature gradients result in degradation and mechanical gradients. They also contribute to involve unique deformation mechanism within the laminates' plies depending on the mechanical loading conditions (tension or compression). Ultimately, along with local thermal loading, laminates experience atypical failure modes. The purpose of the present section is to investigate the failure mechanisms associated with local fire exposure in order to correlate these damages with the structural integrity of CG/PEEK laminates. The same material was tested in the as-received state in tension and in compression at room temperature (Table 1) in a previous work [53].

#### **4.3.1 Tensile behaviour**

In as-received tensile specimens, the mechanical load is primarily borne by the 0° plies, resulting in a fiber-driven behaviour (Figure 7). The 16 plies CG/PEEK plate with a quasi-isotropic lay-up has been exposed to a kerosene flame for different exposure times (5-10-15 min).

Depending on the position of the tensile specimen (directly waterjet cut from the plate) and the exposure time, the macroscopic mechanical response significantly differs from one specimen to



another. From a general standpoint, the mechanical behavior is elastic-brittle in the two specimens far from kerosene flame (specimens #1 and #5). This macroscopic response is very similar to the one observed in as-received state (no prior fire exposure). The tensile response shifts to an elastic quasi-brittle behavior as the distance to kerosene flame decreases (specimens #3 and #4). Specimen #3 seems much degraded with an elastic domain interrupted at 0.3% strain. In addition, the behavior of specimen #2 seems to join that of specimen #4 for 15 minutes of exposure to the flame. It therefore appears that the structural capabilities of the most severely degraded specimens dramatically decrease.

Regardless the exposure time and depending on the position of the tensile specimen cut from the plate exposed to fire, it also appears that the two specimens far from kerosene flame (specimens #1 and #5) are not seemingly degraded for all fire testing conditions. With respect to the as-received specimens, it is therefore expected that the degradation gradient (induced by localized flame exposure) will reflect on the tensile properties of the specimens. The influence of in-plane and through-thickness temperature gradients on the decrease in the tensile properties of CG/PEEK laminates is clearly shown on Figure 8. In specimens #1 and #5, the decreases in both axial stiffness and strength are moderate (about 15%), confirming that thermal degradation is very limited in these specimens. However, in the most degraded state (specimen #3), as was suggested by the macroscopic tensile response, the axial stiffness dramatically decreases by almost 50% and the axial strength loses 70% of its initial value (as-received state). The kerosene flame exposure time is also instrumental in ruling the magnitude of in-plane and through-thickness temperature gradients and subsequent mechanical properties. The decrease in tensile stiffness is similar for all specimens taken from plates exposed to kerosene flame for 300 to 900 s (Figure 8). Surprisingly, it appears that fire exposure time (in the range of studied times) has no significant influence on the axial stiffness. Indeed, the latter tends to stabilize after a 300 s exposure though the extensively degraded area increases as exposure time increases (Figures 5 and 6). As far the tensile strength is concerned, the 900 s exposure case slightly differs as Figures 5 and 6 clearly show that the in-plane and through-thickness degraded areas are larger. Ultimately, the tensile strength of specimens #2 and #4 tends to the value of specimen #3.

These results will be now discussed along with the observations of failed specimens in tension. First, the failure in tension of specimens far from kerosene flame (specimens #1 and #5) is characterized by the breakage of 0° fibers (Figure 9), similarly to what was observed in as-received specimens [53]. Furthermore, the specimens localized in the kerosene flame area are characterized by two well-defined areas: (1) a more or less extensively delaminated (close to the exposed surface) – (2) an area with little damage (close to the back surface). More specifically, along with the observations of the thermally degraded CG/PEEK plates (Figures 5-6), the observations of the most degraded specimen #3 after tensile loading (Figure 10) shows that the exposed surface is characterized by the thermal decomposition of the PEEK matrix after 300 and 600 s exposure. It results in the formation of

carbonaceous char as well as the complete ablation of the G/PEEK outer ply after a 900 s flame exposure.

From the mechanical behavior standpoint, it therefore suggests that the structural integrity of the exposed ply is significantly affected. In addition, the adjacent plies underneath the exposed surface being severely delaminated, it also means that the tensile load cannot be transferred to these adjacent plies once the breakage of  $0^\circ$  fibers occurs. The barrier formed by extensive delamination contributes to relatively preserve the structural integrity of the plies close to the back surface. In other words, the tensile load borne by  $0^\circ$  plies is expected to differ in the two well-defined areas of the quasi-isotropic laminates, and most of the mechanical load is borne by the less damaged area. Thus, the tensile load is taken up by the  $0^\circ$  fibers plies in the non-delaminated area (Figure 9). Ultimately, the relatively well-preserved plies close to the back surface are characterized by the gradual breakage of  $0^\circ$  fibers plies (Figure 10). These failure mechanisms are also revealed by the successive drops of the tensile load as evidenced on the stress-strain curves of the most degraded specimens (Position #3 in Figure 7). In the quasi-isotropic  $[(0/90)_V,(0/90),(\pm 45),(0/90),(\pm 45),(0/90),(\pm 45),(0/90)]_S$  laminates investigated here, one also may notice that the number of drops is somehow correlated to the thickness of the non-delaminated area and the number of  $0^\circ$  plies.

As indicated in section 4.2, the non-delaminated area represents about half the laminates thickness after 5- and 10-minutes flame exposure. After a 15 min exposure, the non-delaminated area represents about 1/3 of the laminates thickness. In the specimens exposed for 5 min, six drops are observed in the tensile response, what may correspond to the breakage of 6 plies oriented at  $0^\circ$ . In the specimens exposed for 10 and 15 min, 4 and 2 drops are observed, respectively. The macroscopic tensile responses of specimens #3 under different flame exposure times (Figure 7) also suggest that once the  $0^\circ$  fibres plies are broken, the  $\pm 45^\circ$  plies tends to take up the tensile load. It results in shifting the fracture behavior from brittle (sudden breakage of  $0^\circ$  fibers plies) to ductile. As exposure time increases, the gradual failure of most degraded specimens subjected to a tensile loading comes along with the plastic deformation of  $\pm 45^\circ$  plies as well as fiber/matrix debonding and delamination (Figure 11b). Microscopic observations done on the most degraded specimen in central position (Figure 11) clearly emphasize at small scale the two well-defined areas that play different roles from both thermal and mechanical responses, as was previously mentioned. A closer look to the exposed surface shows the influence of flame exposure time on the thermal decomposition of the PEEK matrix. The complete pyrolysis of the matrix is reached after 15 min and the microscopic observations reveal a network of dry fibers on the exposed surface.

#### **4.3.2 Compressive behaviour**

The geometry of compressive specimens (100x150 mm<sup>2</sup>) complies with the test standard (see section 3.3) aiming at determining the compressive strength after impact of laminated composites [43]. Compressive tests on kerosene flame exposed specimens are therefore derived from the localized damage induced by impact [13][43-44]. As a result, the compressive mechanical properties (equivalent stiffness and strength) derived from these tests cannot be relevantly compared to the ones obtained from the conditions applied along with the compressive test European standard EN 2850 [53]. Indeed, the compressive axial stiffness and strength are  $E_x = 49.25 \text{ GPa}$  and  $\sigma_x^u = 573 \text{ MPa}$ , respectively (Tab. 1). Theoretically, it therefore means that a 260 kN compressive load would be necessary to observe the ultimate failure of 100x150 mm<sup>2</sup> specimens. It was not possible to perform this test on our testing machine as the maximum load cell capacity is 100 kN. From the macroscopic compressive responses, it appears that CG/PEEK laminates have an elastic-brittle behavior, suggesting that the compressive load is primarily borne by the 0° plies of specimens with a quasi-isotropic stacking sequence (Figure 12a). One may also notice that the macroscopic response is not significantly influenced by the flame exposure time. However, flame exposure leads to damage gradients within the laminates (Figures 5 and 6), there are virtually no preliminary sign of damage before ultimate failure in compression. The macroscopic stress-strain curve also suggests that only the 0° plies in the non-delaminated area are capable of bearing the load. These 0° plies are localized along the specimen's edges (Figure 5) as well as on the non-exposed side of the laminates (Figure 5). From the macroscopic compressive properties standpoint (Fig. 12b), it turns out that flame exposure has little influence on the axial stiffness (-10%) and a moderate decrease in axial strength after 15 min exposure (-20%). The influence of flame on the mechanical behavior is now discussed considering the failure modes taking place in compression.

Failure modes in laminates whose mechanical behavior is driven by fibers (for instance in quasi-isotropic laminates) typically include breakage of 0° fibers, splaying, wedging, kink bands (buckling at both microscopic and macroscopic scales). As was discussed in the tensile loading case, the two well-defined areas induced by flame exposure (Figures 5 and 6) are expected to reflect on failure modes in compression. In severely delaminated composites laminates (which is the case here) subjected to a compressive loading, buckling is expected to play a prominent role. Finite Elements calculations were conducted on the as-received material in a previous study [54], to account for the compressive response of 100x150 mm<sup>2</sup> as the ones used in the present work. From simulations, it turns out that the first buckling mode to appear is the mode 2 buckling (2 blisters of opposite direction) at about 360 MPa and the mode 1 buckling (1 blister) appears shortly after at about 380 MPa (the mode 3 buckling appears much later at about 500 MPa). A prior flame exposure contributing to create delamination and out-of-plane displacements of the plies within the laminates (as shown in Fig. 6), one may reasonably assume that local buckling will appear at lower stresses in thermally damaged plies, though it is not possible to estimate the corresponding buckling stresses. In addition, one may also recall that the

present compressive testing is based on anti-buckling knife-edges and clamping blocks whose interest is to prevent the specimen buckling (Figure 4).

Ultimately, the purpose is to promote the breakage of  $0^\circ$  fibers in compression. As expected, Figure 13 shows that the two well-defined areas induced by flame exposure result in modifying the stress distribution within the laminates. As the compressive load cannot be borne by the delaminated plies near the exposed surface, it is transferred to the virtually undamaged areas on the backside of the specimen as well as along the edges outside the kerosene flame degraded area. Thus, the compressive load is taken up by the  $0^\circ$  fibers in non-delaminated areas of the specimens.

Once the compressive strength is reached in these areas, the through-thickness breakage of  $0^\circ$  fibers is observed (Figure 14), leading to the transverse cracking of the specimen. A Digital Image Correlation technique is applied to the back surface of the specimen (the less damaged one) during compressive loading. The evolution of the axial strain distribution with time reveals that transverse cracking comes along with the formation of a plastic kink band initiated in the delaminated area localized in the kerosene flame degraded area (Figure 13). This buckling band is associated with the localization of positive axial strains whereas the upper and lower areas of the specimen are in compression (negative values of the axial strain). Regardless the flame exposure time, the observations of the right- and left-hand sides of laminates edges clearly emphasize these damage mechanisms. The formation of the plastic kink band ultimately results in the breakage of  $0^\circ$  fibers either in the form of wedging or a shearing band (Figure 14). The dimensions of the degraded area on the exposed surface (Figure 5) and the extension of delaminated areas within the laminates (Figure 6) gradually increase along with the flame exposure time. Conversely, the compressive properties gradually decrease as there are slightly less undamaged areas allowing the  $0^\circ$  fibers to bear the compressive load. However, the reduction of the compressive stiffness and strength is quite moderate after 15 min (-10 and 20%, respectively) with respect to the specimens exposed to a kerosene flame for 5 min. To conclude on the structural integrity of CG/PEEK laminates subjected to compressive loadings, it would be necessary to determine the reference value in the same testing conditions applied to as-received specimens (no prior flame exposure).

#### **4.3.3 Post-fire compressive properties**

The influence of fire-exposure time on the compressive stiffness and failure strength is shown in Fig. 12b. Very little work has been done in the literature when it comes to evaluate the coupling between severe fire exposure (kerosene flame) and the residual mechanical properties of thermoplastic-based composite laminates. Unfortunately, there is no thermal-mechanical coupled simulation available now to explain the complex changes in fire performance along with tensile / compressive mechanical behaviours. However, Mouritz and Mathys have used analytical models for determining the post-fire tension, compression and flexure properties are presented [55]. The potential use of the models for

making preliminary predictions of reductions to the failure loads of glass-reinforced polyester composite structures caused by fire is discussed. A few authors have shown that, due to the low stiffness modulus and high strength, the plate structural integrity is often governed by excessive deformation criteria or local and global buckling criteria in compression [56-58].

In the present study, the compressive failure of CG/PEEK specimens is mainly due to global buckling. Compression tests conducted on specimens that were completely charred in the fire tests revealed that the char layer had no residual compressive stiffness or strength [55]. In other words, this layer is unable to support a compressive load. Thus, this feature needs to be considered to estimate of the ultimate compressive strength given by the compressive buckling load of a fire-damage laminates. By using the theory developed on the buckling of thin plates under uniaxial compression [59], it is known that the critical buckling load  $P_{cr}$  for a plate with fixed edges is defined by:

$$\sigma_{cr} = \frac{K_r D \pi^2}{t b^2}$$

Where:

- $K_r$  is the restraint coefficient accounting for the effect of constraining the plate's edges and whose value depends on the specimen length to width ratio  $r = a/b$ . In the present case  $r = 1.5$  and  $K_r = 8.33$ .
- $D = Et^3/[12(1 - \nu^2)]$  is the flexural stiffness,  $E$  is the compressive modulus,  $\nu$  is the Poisson's coefficient and  $t$  is the laminates' thickness. The compressive modulus of CG/PEEK laminates is  $E = 48.7 \text{ GPa}$  and  $\nu = 0.04$  [54].

Based on these expressions, the critical buckling stress can be re-written as follows:

$$\sigma_{cr} = E \frac{K_r \pi^2}{[12(1 - \nu^2)]} \left(\frac{t}{b}\right)^2$$

In the case of fire-damaged laminates with a charred layer whose thickness is  $t_c$ , the previous equation becomes [55]:

$$\sigma_{cr} = E \frac{K_r \pi^2}{[12(1 - \nu^2)]} \left(\frac{t - t_c}{b}\right)^2$$

This relationship gives theoretical values of the compressive buckling stress at failure that are in rather good agreement with the experimental values (see Fig. 12b), suggesting that the fire-damaged laminates can be considered as a bi-layer material with one layer being the thermally-degraded one (referred to as char layer) and the other layer the underlying "unburnt" material.

## 5. Conclusions

For aeronautical certification purposes, the bearing capabilities of composite materials exposed to kerosene flame aggressions (116 kW/m<sup>2</sup> and 1100 °C) are required to be preserved for 15 min. Most references in literature have addressed the influence of heat flux or kerosene flame only in terms of fire-behavior (thermal response) but not in terms of residual mechanical properties (stiffness and strength). Thus, the question of coupling between thermal decomposition and mechanical behavior in polymer-based laminated composites is still widely opened.

Regardless the exposure time, the kerosene flame exposure involves in-plane and through-thickness temperature gradients, which ultimately create two well-defined areas within the laminates: an extensively delaminated one (the one close to the exposed surface) and a relatively well preserved one (close to the back surface). From the present work, it is possible to conclude that the mechanical properties in tension and in compression are severely affected by prolonged exposures to kerosene flame (15 min) with respect to as-received specimens. In addition, the flame exposure time (ranging from 5 to 15 min) seems to have little very influence on tensile properties and the effect is moderate on compressive properties, with respect to a 5 min exposure.

The barrier formed by an extensive thermally induced delamination contributes to relatively preserve the structural integrity of the plies close to the back surface. In other words, the tensile load borne by 0° plies is expected to differ in the two well-defined areas of the quasi-isotropic laminates, and most of the mechanical load is borne by the less damaged area. However, in the most degraded state (specimen #3), the axial stiffness dramatically decreases by almost 50% and the axial strength loses 70% of its initial value (as-received state). In compression, the influence of flame exposure is more detrimental as the mechanical load cannot be borne by the plies localized in the delaminated area. The compressive load is transferred to the virtually undamaged areas on the backside of the specimen as well as along the edges outside the kerosene flame degraded area. Thus, the compressive load is taken up by the 0° fibers in non-delaminated areas of the specimens.

### **Acknowledgements**

The work presented in this study is the result of the RIN (Réseau d'Intérêt Normand) project AEROFLAMME (Behaviour of **AERO**nautical Composites under **FLAM**me and **ME**chanical Loading) financed by the Normandy Region and the FEDER (European Regional Development Fund).

### **Data Availability Statement**

The data that support the findings of this study are available on request from the corresponding author. The data are not publicly available due to restrictions e.g. their containing information that could compromise the privacy of research participants.

## References

- [1] L. Zhu, N. Li, P.R.N. Childs. Light-weighting in aerospace component and system design. *Propuls. Power Res.* 7, 103–119 (2018).
- [2] A. Saleem, L. Frommann, A. Iqbal. High performance thermoplastic composites: Study on the mechanical, thermal, and electrical resistivity properties of carbon fiber-reinforced polyetheretherketone and polyethersulphone. *Polym. Compos.* 28: 785–796 (2007).
- [3] Vieille B., Albouy W., Chevalier L., Taleb L. About the influence of stamping on thermoplastic-based composites for aeronautical applications. *Compos. Part B Eng.* 45: 821–834 (2013).
- [4] Fujihara, K., Huang, Z.-M., Ramakrishna, S. & Hamada, H. Influence of processing conditions on bending property of continuous carbon fiber reinforced PEEK composites. *Compos. Sci. Technol.* 64, 2525–2534 (2004).
- [5] C. Lu, N. Xu, T. Zheng, X. Zhang, H. Lv, X. Lu, L. Xiao, D. Zhang. The optimization of process parameters and characterization of high-performance CF/PEEK composites prepared by flexible CF/PEEK plain weave fabrics. *Polymers* 11, (2018).
- [6] Chen J., Wang K., Dong A., Li X., Fan X., Zhao F. A comprehensive study on controlling the porosity of CCF300/PEEK composites by optimizing the impregnation parameters. Volume 39, Issue10, October 2018, 3765-3779.
- [7] Vodermayr A.M., Kaerger J. C., Hinrichsen G. Manufacture of high performance fibre-reinforced thermoplastics by aqueous powder impregnation. *Compos. Manuf.* 4, 123–132 (1993).
- [8] Vieille B., Lefevbre C., Coppalle A., Post fire behavior of carbon fibers thermoplastic- and thermosetting-based laminates for aeronautical applications: a comparative study. *Materials and Design*, 63, pp. 56-68, 2013.
- [9] Vieille B., Coppalle A., Keller C., Garda M-R., Viel Q., Dargent E. Correlation between post fire behavior and microstructure degradation of aeronautical polymer composites. *Materials and Design*, 74, pp. 76-85. 2015.
- [10] Carpier Y., Vieille B., Coppalle A., Barbe F. About the tensile mechanical behaviour of carbon fibres fabrics reinforced thermoplastic composites under very high temperature conditions. *Composites Part B*, doi: 10.1016/j.compositesb.2019.107586, 2019.
- [11] Carpier Y., Vieille B., Delpouve N., Dargent E. Isothermal and anisothermal decomposition of Carbon fibres polyphenylene sulfide composites for fire behavior analysis. *Fire Safety Journal*, 109: 102868, 2019.

- [12] Carpier Y., Vieille B., Maaroufi M.A., Coppalle A., Barbe F. Mechanical behavior of carbon fibers polyphenylene sulfide composites exposed to radiant heat flux and constant compressive force. *Composite Structures*, 200, pp. 1-11, 2018.
- [13] Maaroufi M.A., Carpier Y., Vieille B., Gilles L., Coppalle A., Barbe F. Post-fire compressive behaviour of carbon fibers woven-ply Polyphenylene Sulfide laminates for aeronautical applications. *Composites Part B*, 119, pp. 101-113, 2017.
- [14] Vieille B., Coppalle A., Carpier Y., Maaroufi M.A., Barbe F. Influence of the matrix chemical nature on the post-fire mechanical behavior of notched polymer-based composite structures for high temperature applications. *Composites Part B*, 100, pp. 114-124, 2016.
- [15] Schuhler E., Coppalle A., Vieille B., Yon J., Carpier Y. Behaviour of aeronautical polymer composite to flame: A comparative study of thermoset- and thermoplastic-based laminate. *Polymer Degradation and Stability*, 152, pp. 105-115, 2018.
- [16] A.P. Mouritz, A.G. Gibson, *Fire Properties of Polymer Composite Materials. Solid Mechanics and its Applications*, Springer, Dordrecht, 2006.
- [17] Bourbigot S., Delobel R., Duquesne S. *Comportement au feu des composites. Techniques de L'ingénieur AM5330*, 2006.
- [18] Guillaume E. *Modélisation de la décomposition thermique des matériaux en cas d'incendie. Techniques de L'ingénieur SE2066*, 2015.
- [19] P. Chávez Gómez, T. Pelzmann, E. Robert, L.L. Lebel. Evaluation of the fire resistance of protected carbon/epoxy laminates in small-scale experiments. *AIAA Scitech 2019 Forum*, 7-11 January 2019, San Diego, California.
- [20] Standard method ISO 2685, "Resistance to fire in designated fire zones," 1998.
- [21] P. Tranchard, F. Samyn, S. Duquesne, M. Thomas, B. Estèbe, J-L. Montès, S. Bourbigot. Fire behaviour of carbon fibre epoxy composite for aircraft: Novel test bench and experimental study. *Journal of Fire Sciences*, vol. 33, no. 3, pp. 247–266, 2015.
- [22] T. Chazelle, A. Perrier, E. Schuhler, G. Cabot, A. Coppalle. Fire response of a carbon epoxy composite - comparison of the degradation provided with kerosene or propane flames. *Proceedings of the Ninth International Seminar on Fire and Explosion Hazards (ISFEH9)*, pp. 950-958 Edited by Snegirev A., Liu N.A., Tamanini F., Bradley D., Molkov V., and Chaumeix N. Published by Saint-Petersburg Polytechnic University Press ISBN: 978-5-7422-6498-9 DOI: 10.18720/spbpu/2/k19-17.
- [23] S. LeNeve. AC 20-135 / ISO 2685 Fire tests on components used in fire zones. Comparison of gas burner to oil burner. *International Aircraft Materials Fire Test WG*, Atlantic City, 2008.
- [24] S. I. Stoliarov, S. Crowley, R. E. Lyon, G. T. Linteris. Prediction of the burning rates of non-charring polymers. *Combustion and Flame*, vol. 156, no. 5, pp. 1068–1083, 2009, doi: 10.1016/j.combustflame. 2008.11.010.



- [25] N. Grange, B. Manescau, K. Chetehouna, N. Gascoin. Fire resistance of carbon-based composite materials under both ideal and realistic normative configurations. *Applied Thermal Engineering* 159 (2019) 113834.
- [26] Gascoin N. Experimental study of the burn-through resistance of aeronautical polymer composite materials in case of fire event. 14<sup>th</sup> International Conference and Exhibition on Fire Science and Engineering, Royal Holloway College, UK, 4-6 July 2016.
- [27] S. Timme, V. Trappe, M. Korzen, B. Schartel. Fire stability of carbon fiber reinforced polymer shells on the intermediate-scale. *Composite Structures*, Volume 178, 2017, Pages 320-329.
- [28] Y.M. Ghazzawi, A.F. Osorio, M.T. Heitzmann. The effect of fibre length and fibre type on the fire performance of thermoplastic composites: The behaviour of polycarbonate as an example of a charring matrix. *Construction and Building Materials*, 234, 2020, doi: 10.1016/j.conbuildmat.2019.117889.
- [29] P. Tadini, N. Grange, K. Chetehouna, N. Gascoin, S. Senave, I. Reynaud. Thermal degradation analysis of innovative PEKK-based carbon composites for high-temperature aeronautical components. *Aerospace Science and Technology*, Volume 65, 2017, Pages 106-116.
- [30] N. Grange, P. Tadini, K. Chetehouna, N. Gascoin, I. Reynaud, S. Senave. Determination of thermophysical properties for carbon-reinforced polymer-based composites up to 1000°C. *Thermochimica Acta*, Volume 659, 2018, Pages 157-165.
- [31] N. Grange, P. Tadini, K. Chetehouna, N. Gascoin, I. Reynaud, G. Bouchez, S. Senave, I. Reynaud. Experimental determination of fire degradation kinetic for an aeronautical polymer composite material. *International Journal of Structural Integrity*, <https://doi.org/10.1108/IJSI-03-2017-0021>.
- [32] K. Chetehouna, N. Grange, N. Gascoin, L. Lemée, I. Reynaud, S. Senave. Release and flammability evaluation of pyrolysis gases from carbon-based composite materials undergoing fire conditions, *Journal of Analytical and Applied Pyrolysis*, Volume 134, 2018, Pages 136-142.
- [33] N. Grange, K. Chetehouna, N. Gascoin, S. Senave. Numerical investigation of the heat transfer in an aeronautical composite material under fire stress, *Fire Safety Journal*, Volume 80, 2016, Pages 56-63.
- [34] Westover CM. The Compressive Behavior of Glass Fiber Reinforced Composites Subjected to Local Thermal Loading. Master's thesis, California University at Berkeley, 2000.
- [35] Summers PT, Lattimer BY, Case SW. Compressive failure of composite plates during one-sided heating. *Compos Struct* 2011; 93:2817–25.
- [36] Burns LA, Feih S, Mouritz AP. Compression Failure of Carbon Fiber-Epoxy Laminates in Fire. *J Aircr* 2010; 47:528–33.
- [37] Bausano JV, Lesko JJ, Case SW. Composite life under sustained compression and one-sided simulated fire exposure: characterization and prediction. *Compos Part Appl Sci Manuf* 2006; 37:1092–100.

- [38] Boyd SE, Lesko JJ, Case SW. Composite life under fire sustained compression and one-sided simulated fire exposure: Characterization and prediction. *Compos Sci Technol* 2007; 67:3187–95.
- [39] Feih S, Mouritz AP, Mathys Z, Gibson AG. Tensile strength modeling of glass fiber polymer composites in fire. *J Compos Mater* 2007;41:2387–410.
- [40] Feih S, Mouritz AP. Tensile properties of carbon fibres and carbon fibre–polymer composites in fire. *Compos Part Appl Sci Manuf* 2012;43:765–72.
- [41] A. Hörold, B. Schartel, V. Trappe, M. Korzen, J. Bünker. Fire stability of glass-fibre sandwich panels: The influence of core materials and flame-retardants, *Composite Structures*, Volume 160, 2017.
- [42] C.A. Ulven, U.K. Vaidy. Impact response of fire damaged polymer-based composite materials. *Composites Part B*; 39 : 92–107 (2008).
- [43] Test standard AITM 1.0010. AITM Airbus Ind Test Method, Determination of compression strength after impact., 1994.
- [44] A. Petit, B. Vieille, A. Coppalle, F. Barbe, M.-A. Maaroufi. High temperature behaviour of PPS-based composites for aeronautical applications: Influence of fire exposure on tensile and compressive behaviors. 20<sup>th</sup> International Conference on Composite Materials (ICCM20), Copenhagen, 19-24 July 2015.
- [45] E. Schuhler, B. Lecordier, J. Yon, G. Godard, and A. Coppalle, “Experimental investigation of a low Reynolds number flame jet impinging flat plates,” *International Journal of Heat and Mass Transfer*, vol. 156, p. 119856, 2020.
- [46] E. Schuhler, A. Chaudhary, B. Vieille, A. Coppalle. Fire behaviour of composite materials using kerosene burner tests at small-scales. *Fire Safety Journal*, doi: 10.1016/j.firesaf.2021.103290
- [47] Test standard EN 6035, aerospace series - fiber-reinforced plastics - test method - determination of notched and unnotched tensile strength; Published by the European association of aerospace industries (AECMA), (1996).
- [48] B. Vieille, V.M. Casado, C. Bouvet. Influence of matrix toughness and ductility on the compression-after-impact behavior of woven-ply thermoplastic- and thermosetting-composites: A comparative study. *Composite Structures* 2014, 110: 207-218.
- [49] G. Vanden Poel, Vincent B.F. Mathot. High-speed/high performance differential scanning calorimetry (HPer DSC): Temperature calibration in the heating and cooling mode and minimization of thermal lag. *Thermochimica Acta* 2006; 446: 41–54.
- [50] P. Patel, T.R. Hull, R.W. McCabe, D. Flath, J.G.M. Percy. Mechanism of thermal decomposition of poly(ether ether ketone) (PEEK) from a review of decomposition studies. *Polymer Degradation and Stability* 2010, 95(5): 709-718.
- [51] Lee SM. *Handbook of Composite Reinforcements*. VCH Publishers Inc., 1993: 46.

- [52] Eibl S. Influence of carbon fibre orientation on reaction-to-fire properties of polymer matrix composites. *Fire Mater.* 2012 ; 36 :309–324.
- [53] B. Vieille, J.-D. Pujols Gonzalez, C. Bouvet. Prediction of the ultimate strength of quasi-isotropic TP-based laminates structures from tensile and compressive fracture toughness at high temperature. *Composites Part B* 2019, 164: 437-446.
- [54] N. Dubary, G. Taconet, C. Bouvet, B. Vieille. Influence of temperature on the impact behavior and damage tolerance of hybrid woven-ply thermoplastic laminates for aeronautical applications. *Composite Structures* 2017, 168: 663-674.
- [55] A.P. Mouritz, Z. Mathys. Post-fire mechanical properties of glass-reinforced polyester composites. *Composites Science and Technology* 2001; 61(4): 475-490.
- [56] D. B. R. Babu, V. Prasad, G. Yadav. Analysis of the Flexural Behaviour of Glass Fiber-Reinforced Plastic. *Int Journal of Innovative Research in Science, Engineering and Technology* 2017; 6(10): 19374-19383.
- [57] P. Gu, R.J. Asaro. Structural buckling of polymer matrix composites due to reduced stiffness from fire damage. *Composite Structures* 2005; 69(1): 65-75.
- [58] B.K. Kandola, L. Krishnan, J.R. Ebdon, P. Myler. Structure-property relationships in structural glass fibre reinforced composites from unsaturated polyester and inherently fire-retardant phenolic resin matrix blends. *Composites Part B* 2020; 182: 107607.
- [59] D.W.A. Rees. *Mechanics of Optimal Structural Design: Minimum Weight Structures*. Published by John Wiley & Sons, Ltd, October 2009. doi:10.1002/9780470749784

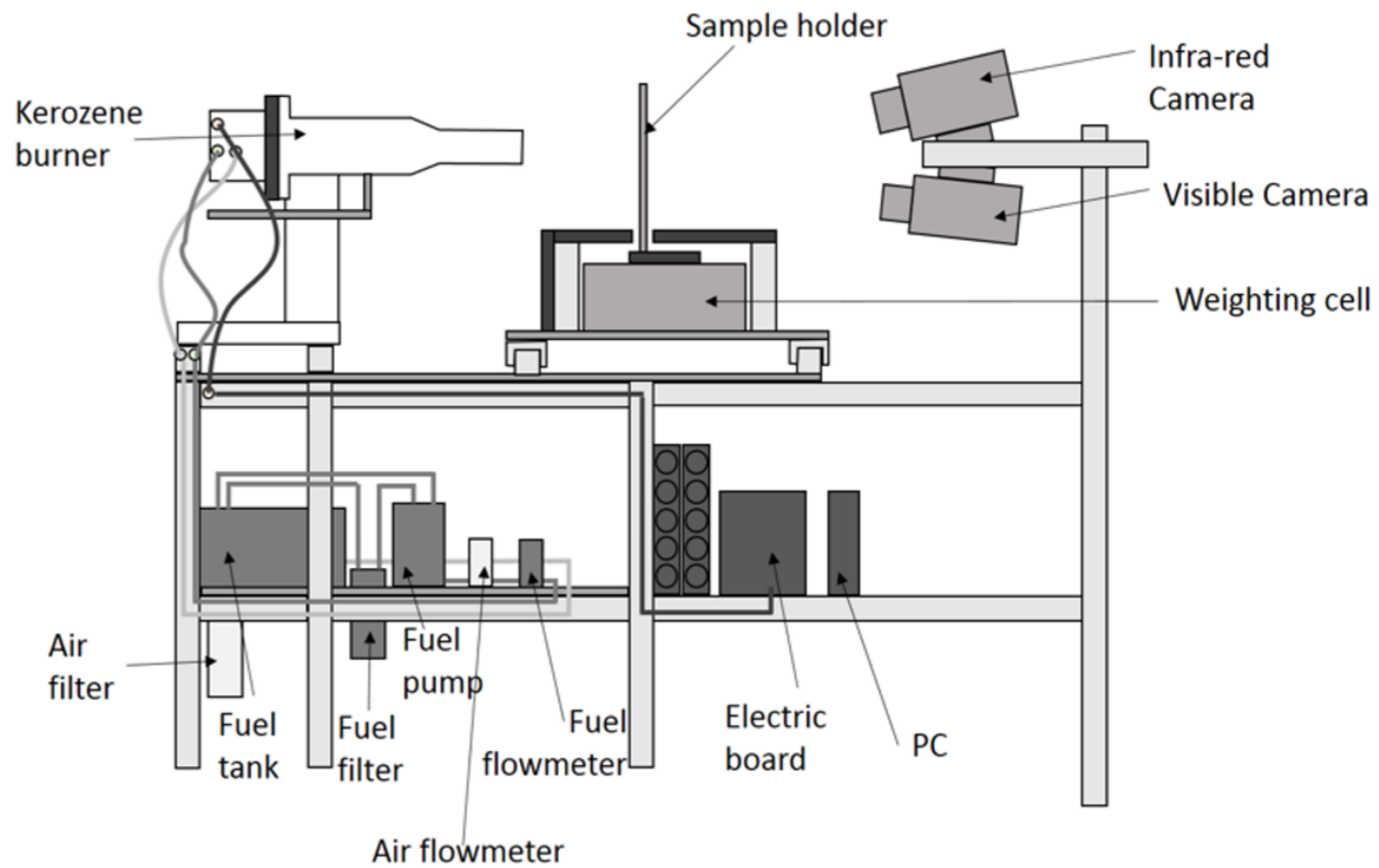
## List of figures

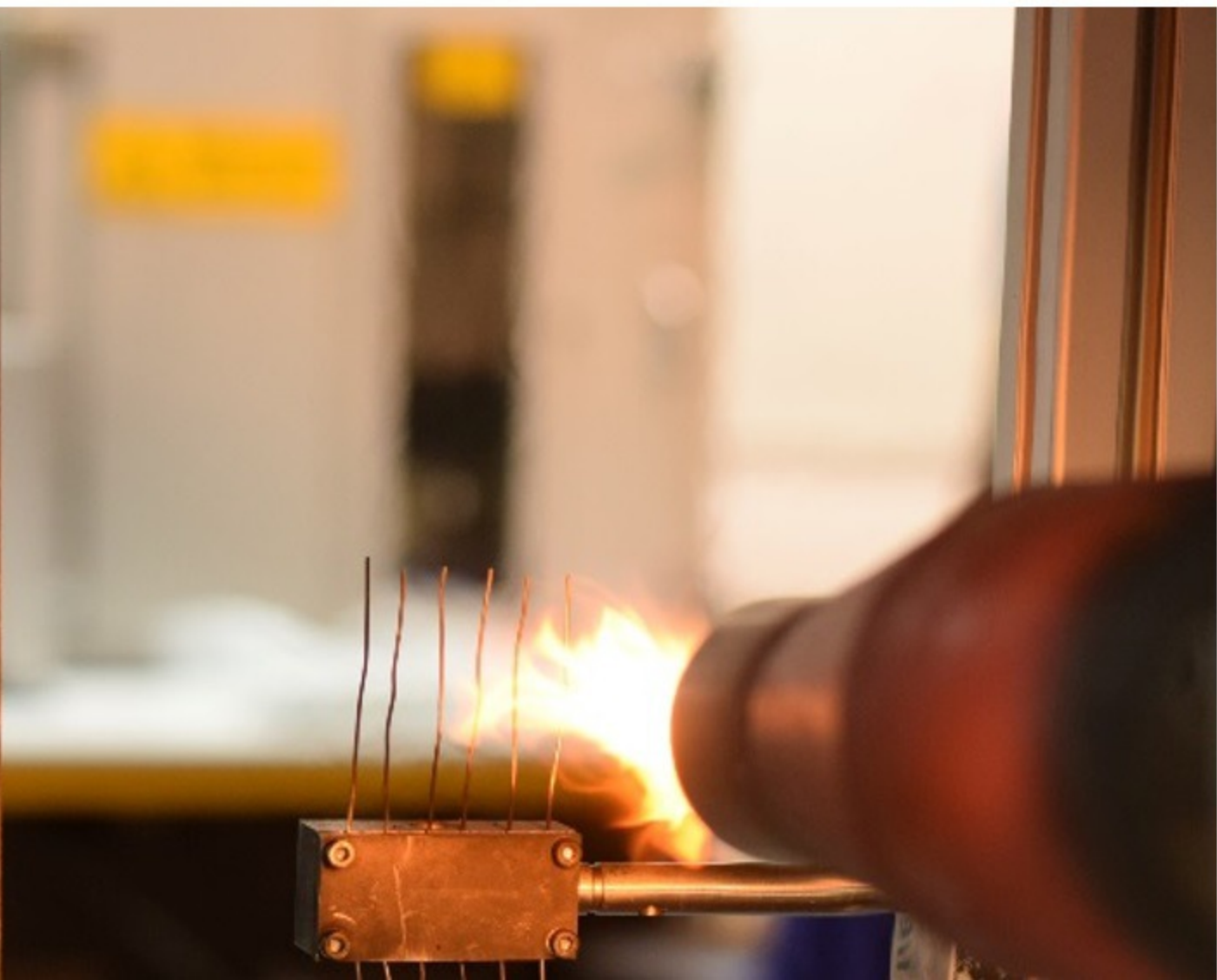
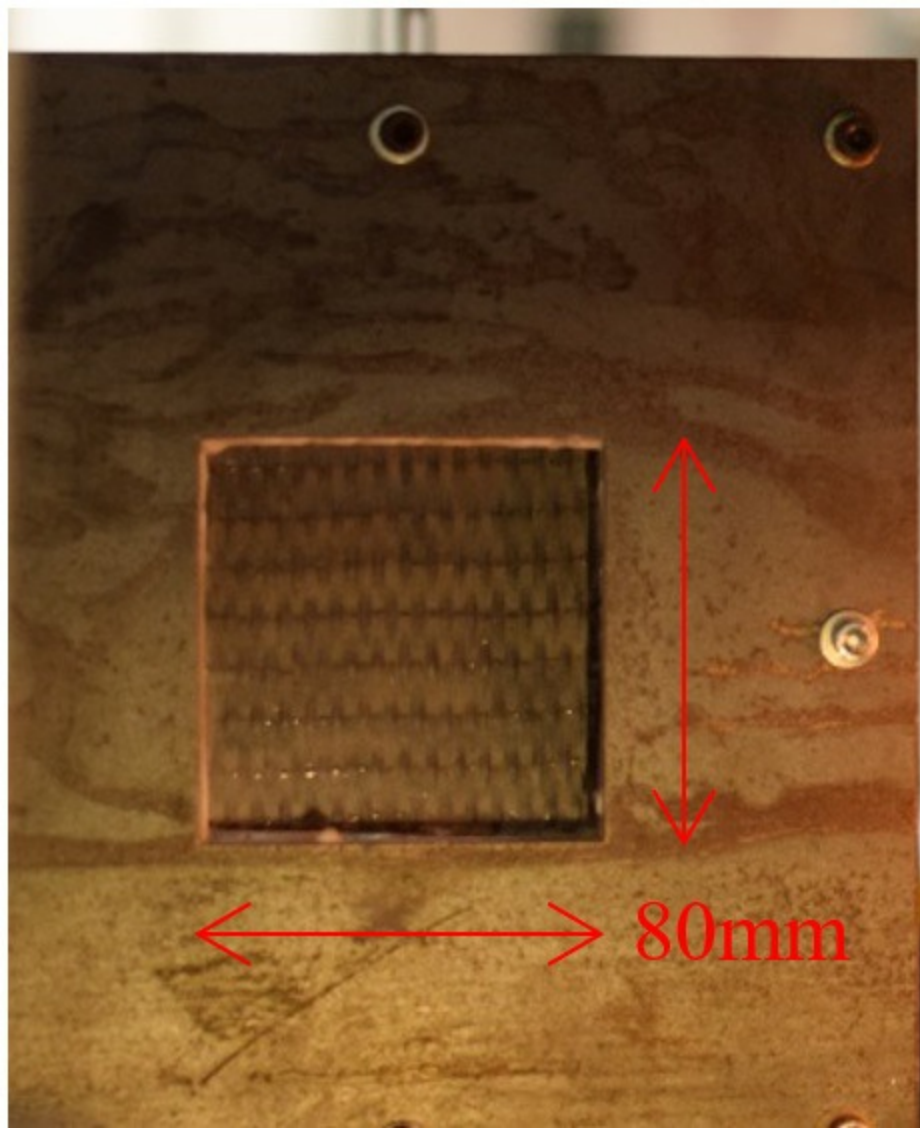
- Fig. 1 – Kerosene flame exposure: (a) Picture of the experimental set-up device - (b) Schematic representation of the kerosene burner bench
- Fig. 2 – Observations of the sample holder on the kerosene flame exposed surface
- Fig. 3 – Compression after kerosene flame exposure tests: (a) experimental set-up and anti-buckling fixture – (b) in situ configuration of the compressive specimen
- Fig. 4 – Influence of heating rate on the thermal decomposition of CG/PEEK specimens by means of TGA under N<sub>2</sub>: (a) Sample mass vs. temperature – (b) Heating rate dependencies of the onset of thermal decomposition, i.e., the temperature for which the sample mass is 95% of its initial mass, and of the residual mass at T = 700 °C
- Fig. 5 – Macroscopic observations of CG/PEEK laminates subjected to kerosene flame for different exposure times: (a) Exposed surface – (b) Back surface
- Fig. 6 – Through-thickness macroscopic observations of CG/PEEK laminates subjected to kerosene flame for different exposure times
- Fig. 7 – Macroscopic tensile responses of CG/PEEK laminates subjected to kerosene flame for different exposure times: (a) 5 min – (b) 10 min – (c) 15 min
- Fig. 8 – Changes in the tensile properties as a function of the kerosene flame exposure time: (a) Axial stiffness – (b) Axial strength
- Fig. 9 – Macroscopic observations of the CG/PEEK laminates after kerosene flame exposure (a) or after tensile testing (b)
- Fig. 10 – Failure in tension of the CG/PEEK specimens (most degraded specimen in central position): (a) Front surface observation – (b) Through-thickness observation
- Fig. 11 – Microscopic observations of failure in tension of the CG/PEEK specimens (most degraded specimen in central position): (a) Front surface observation – (b) Through-thickness observation
- Fig. 12 – Compressive behavior of CG/PEEK laminates subjected to kerosene flame for different exposure times: (a) Macroscopic compressive responses – (b) Changes in compressive properties (axial stiffness and strength)
- Fig. 13 – Exposed and back surfaces observations of the failure modes in compression of the CG/PEEK laminates subjected to kerosene flame for different exposure times – correspondence with the axial strain field obtained from DIC technique: (a) 5 min – (b) 10 min – (c) 15 min
- Fig. 14 – Through-thickness observations of the failure modes in compression of the CG/PEEK laminates subjected to kerosene flame for different exposure times: (a) 5 min – (b) 10 min – (c) 15 min

(a)



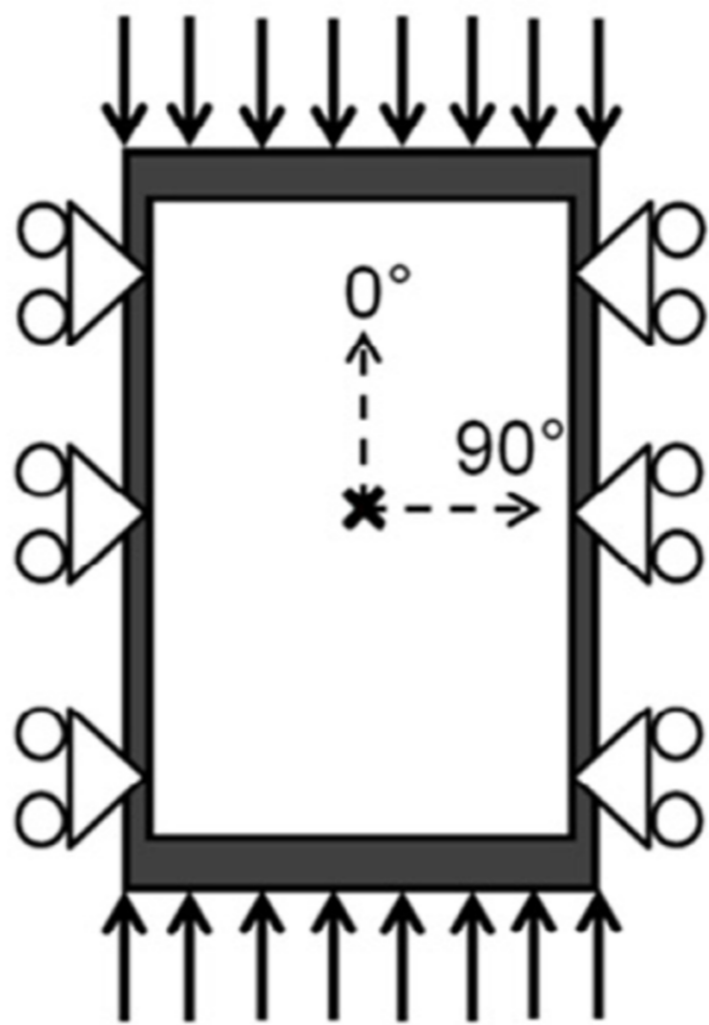
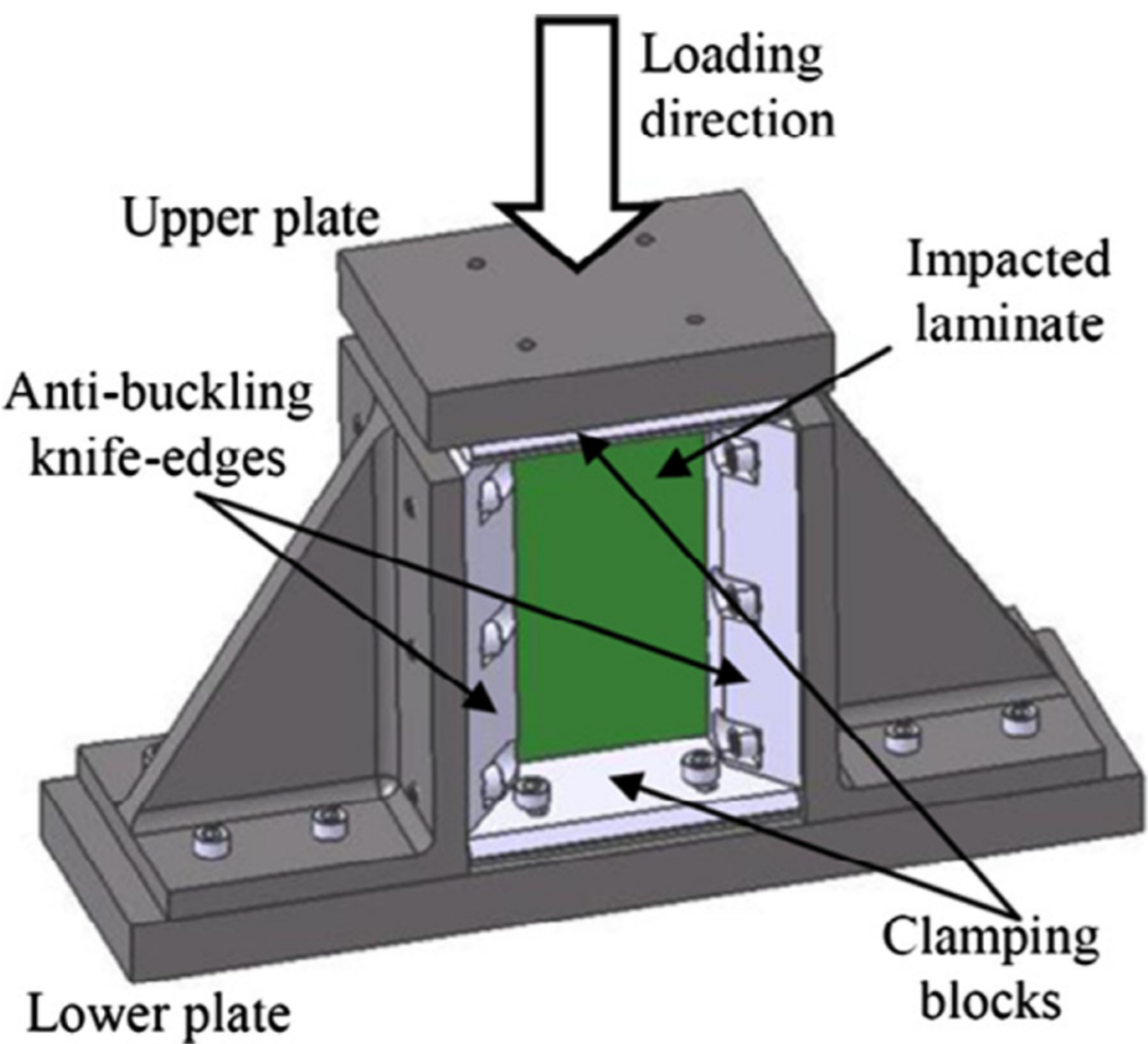
(b)



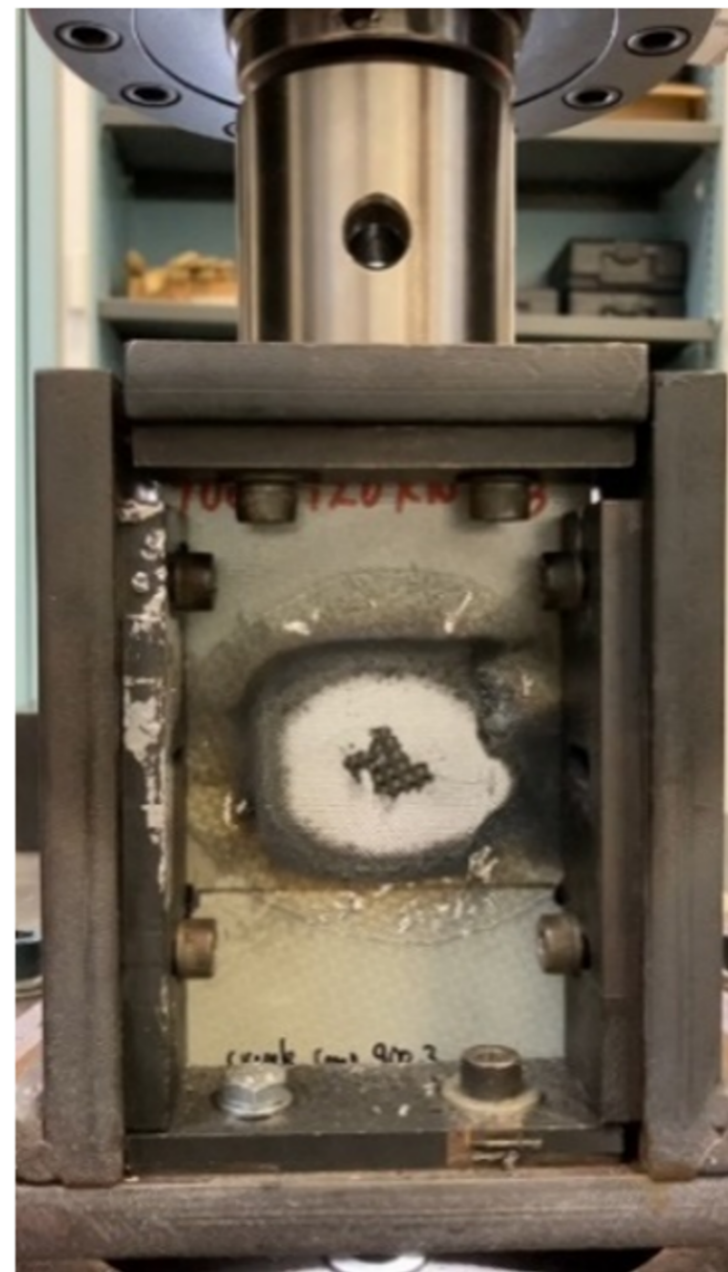




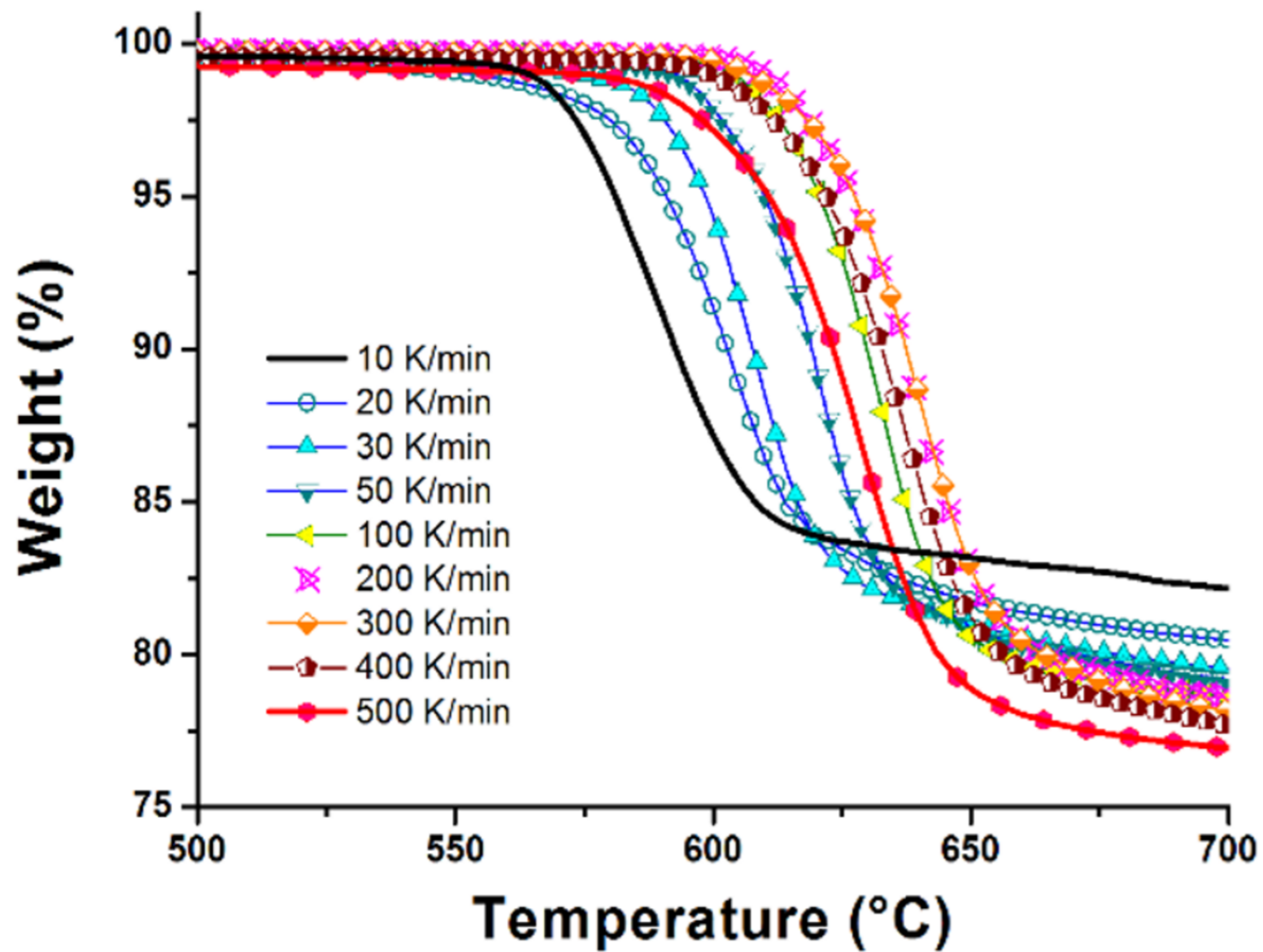
(a)



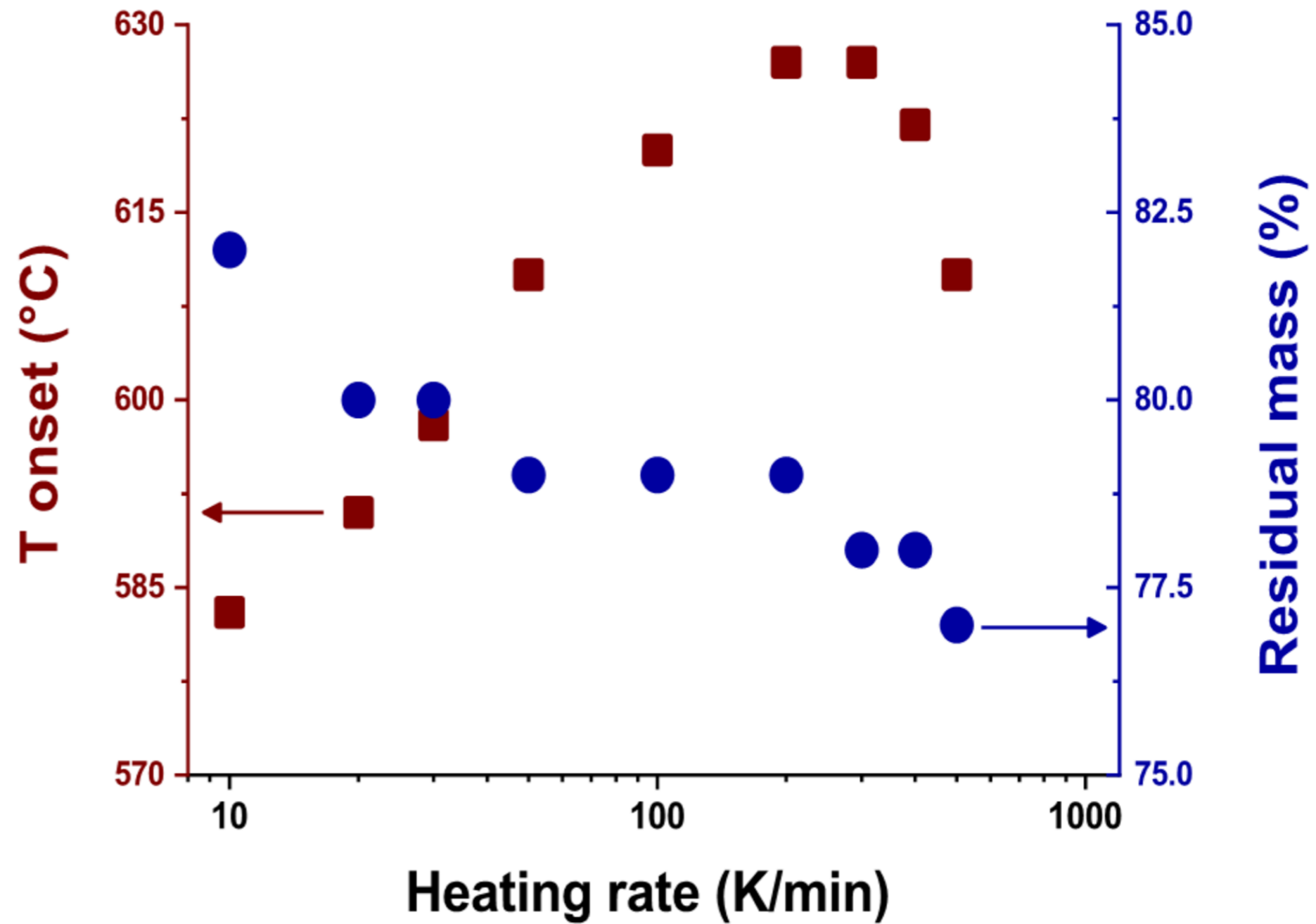
(b)



(a)



(b)



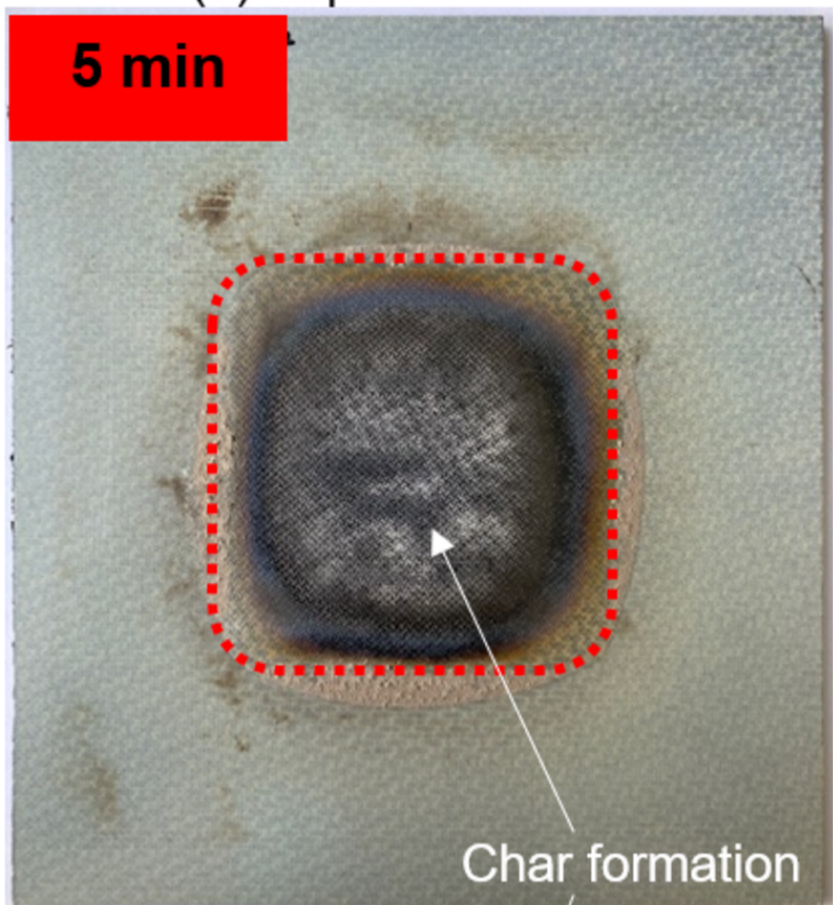


(a) Exposed surface

(b) Back surface

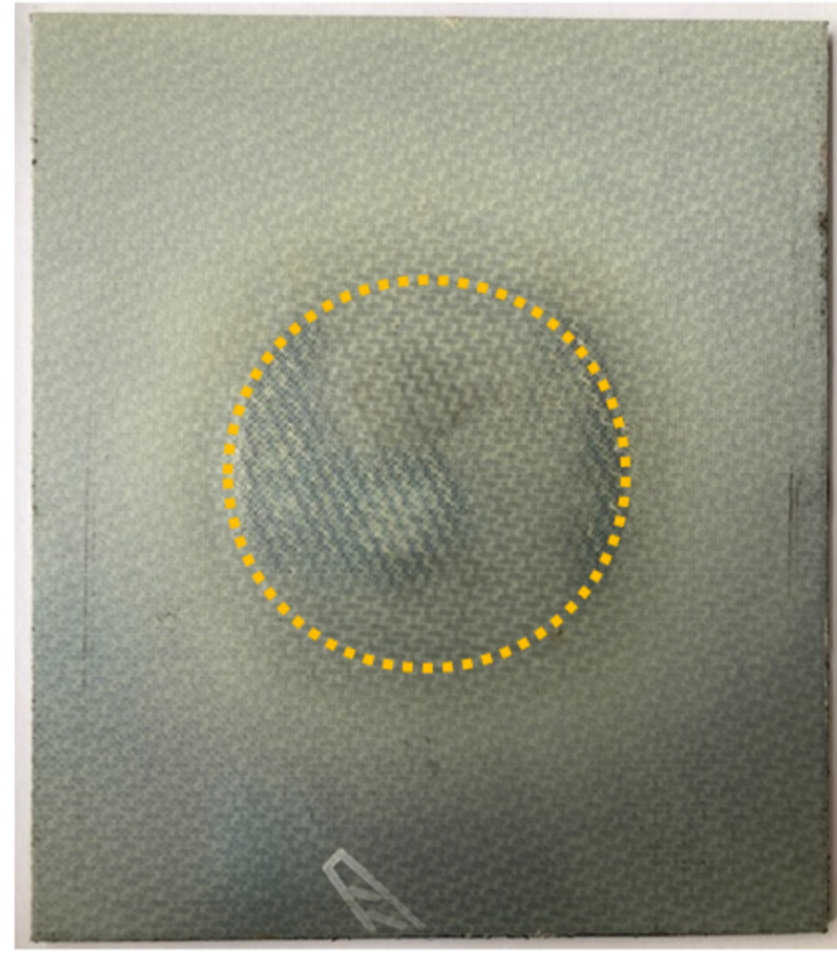
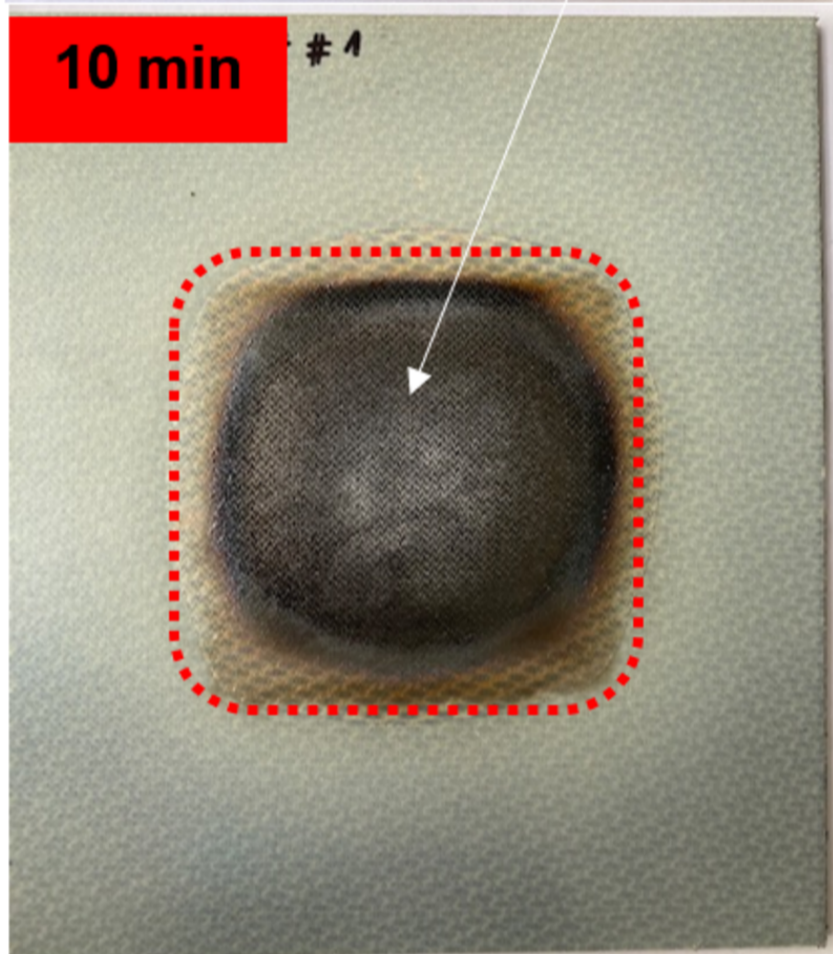
15 mm

5 min

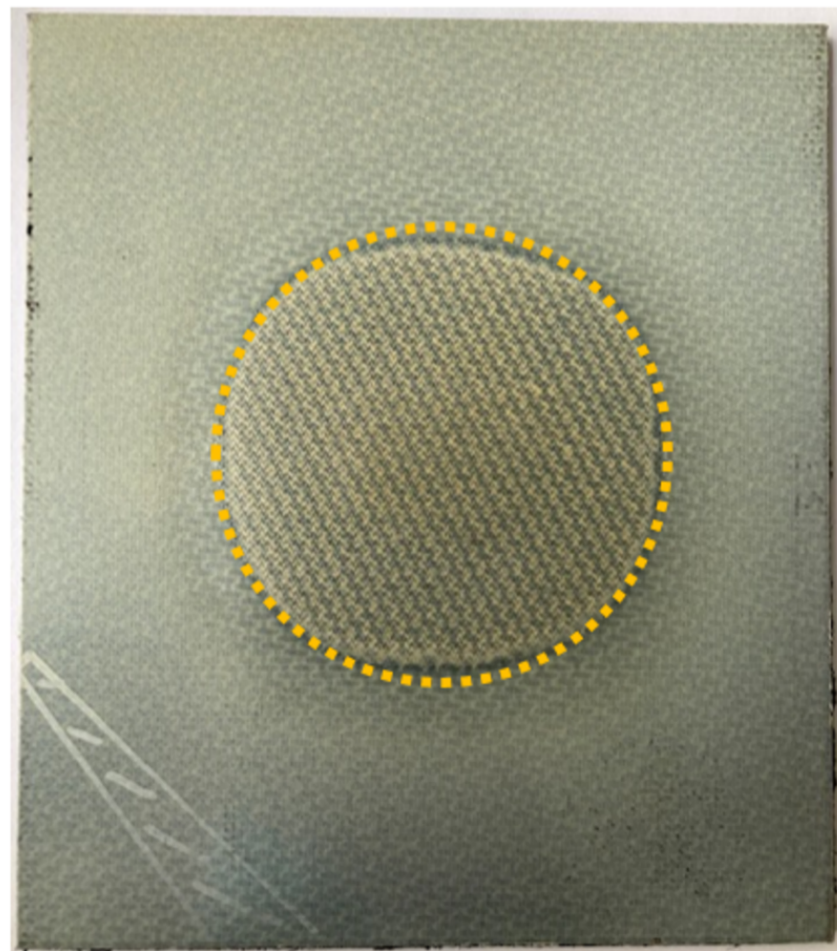
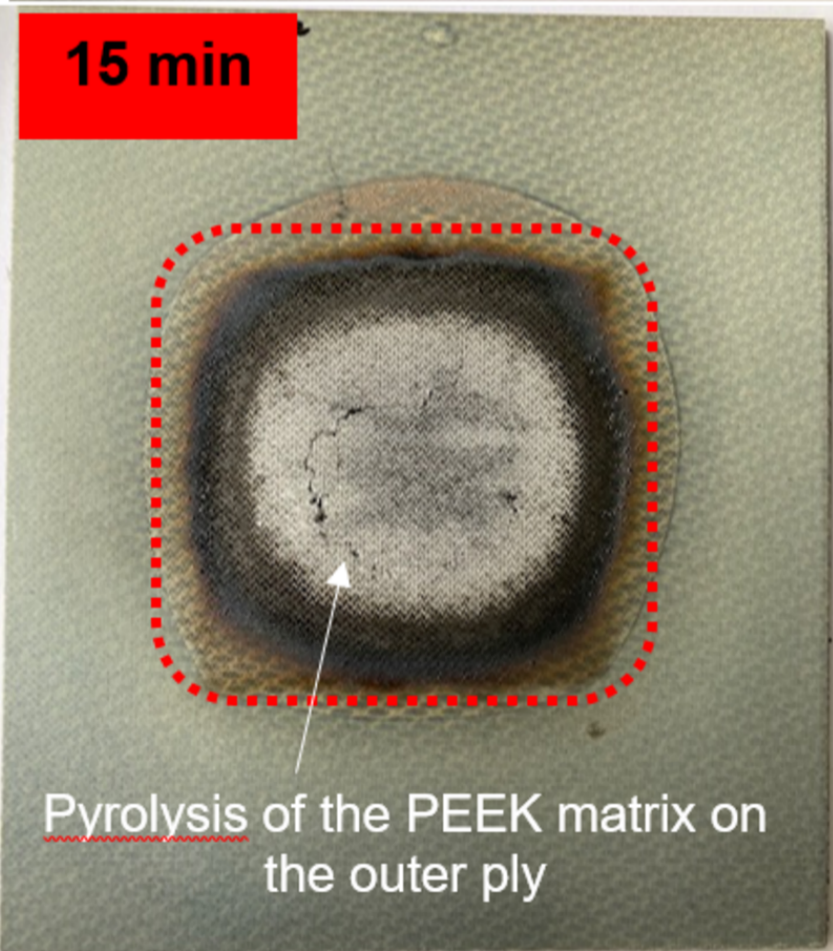



10 min


# 1



15 min



 Kerosene flame degraded area

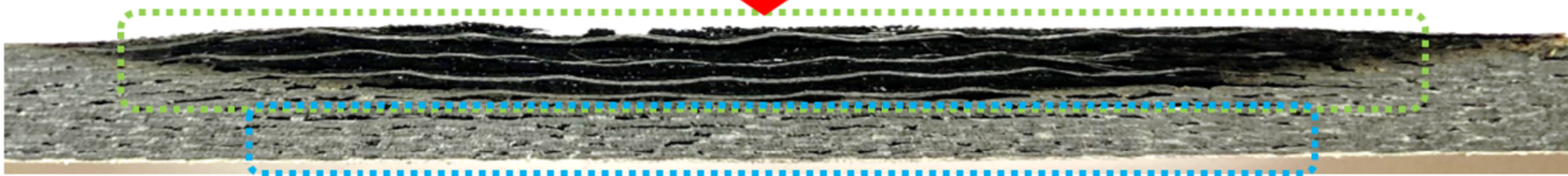
 Melt matrix area



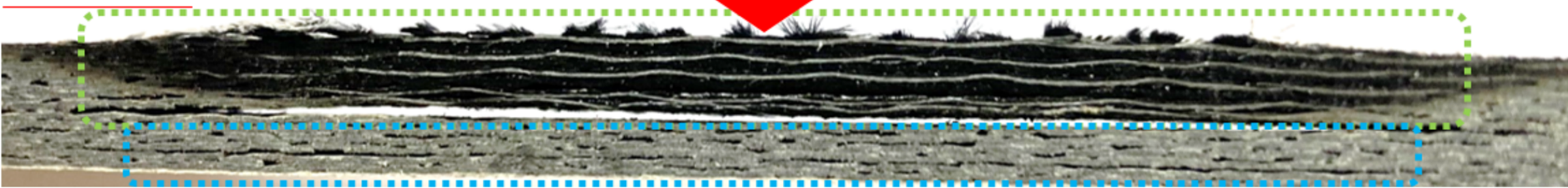
Kerosene flame



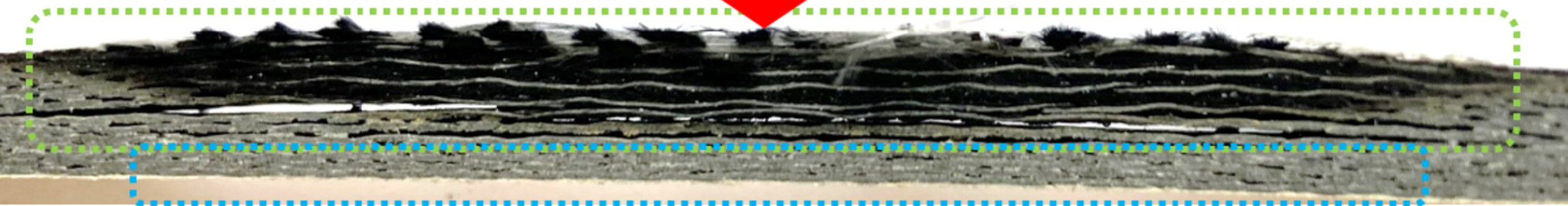
5 min





10 min




15 min



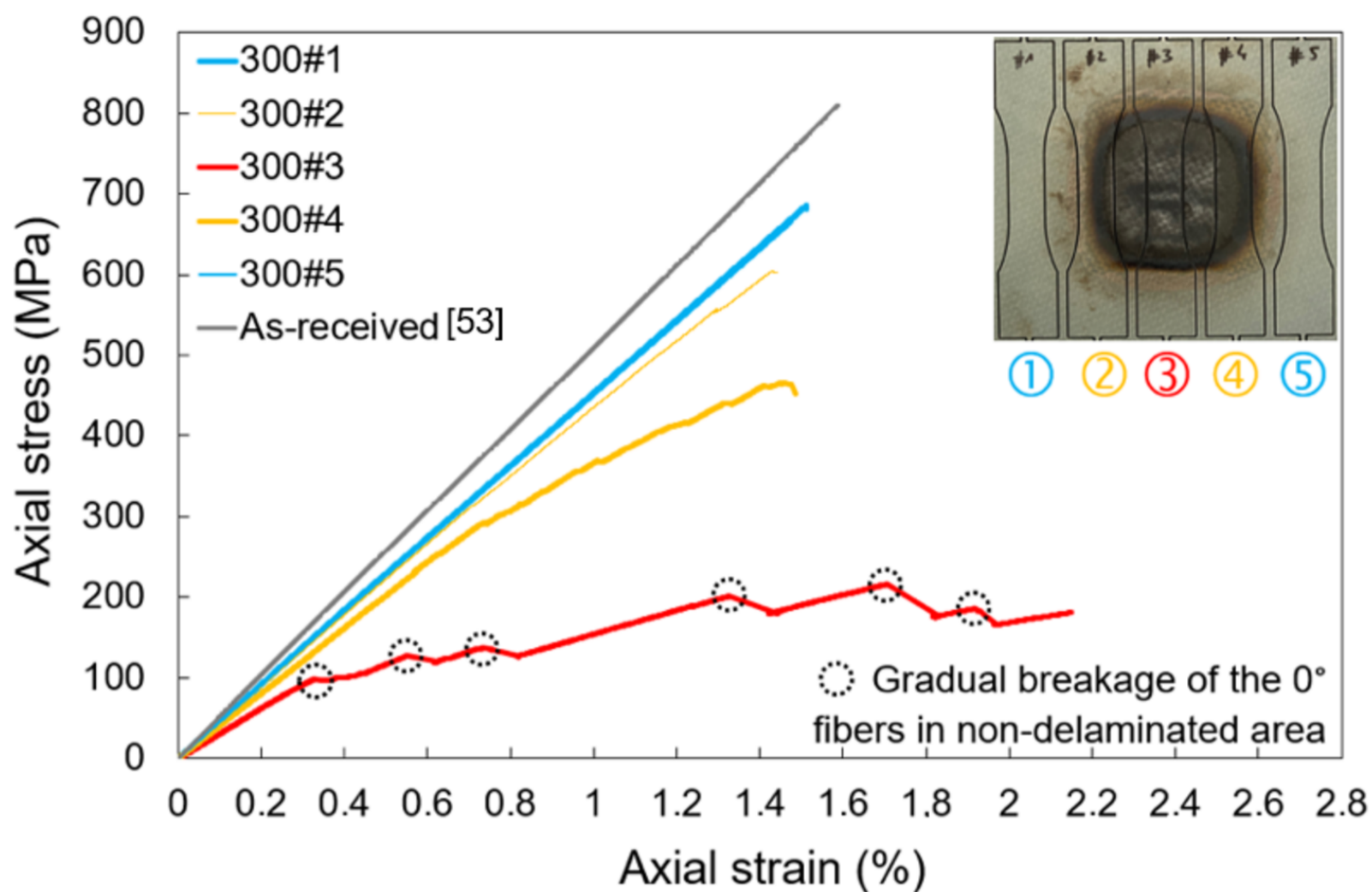
 Extensively delaminated area

 Area with little damage  
(Some intra and interlaminar cracks)

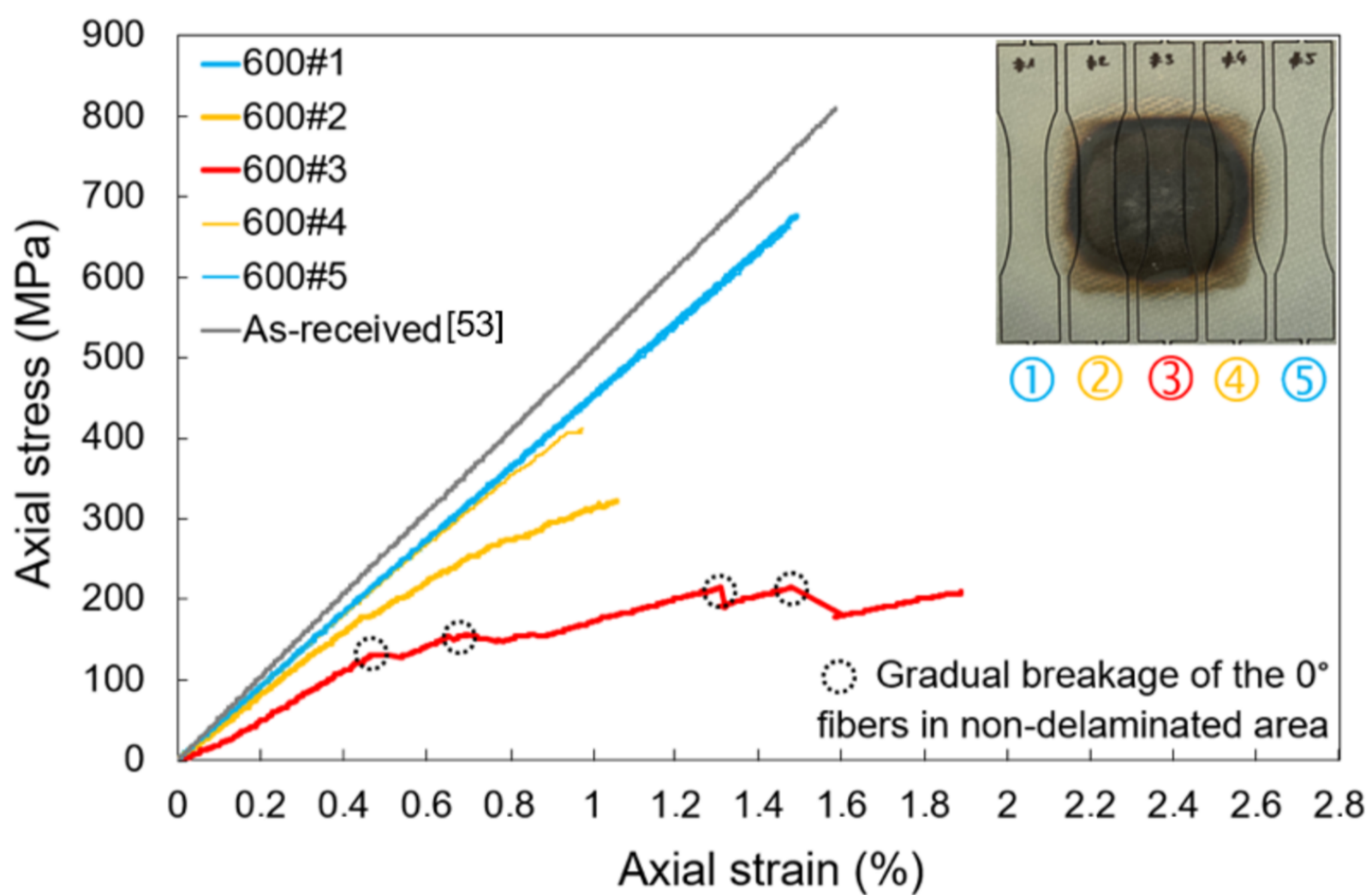
4 mm 



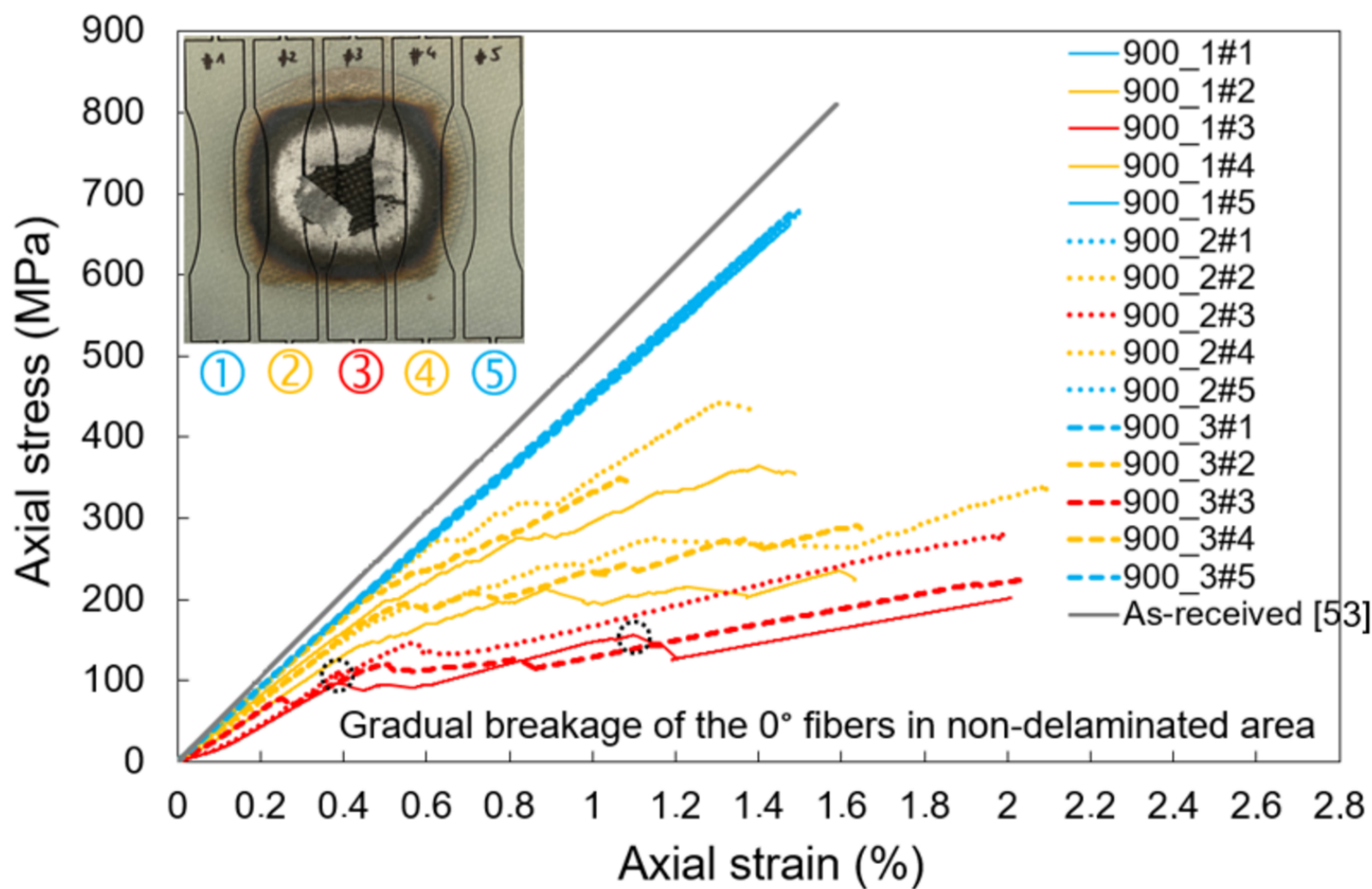
(a)

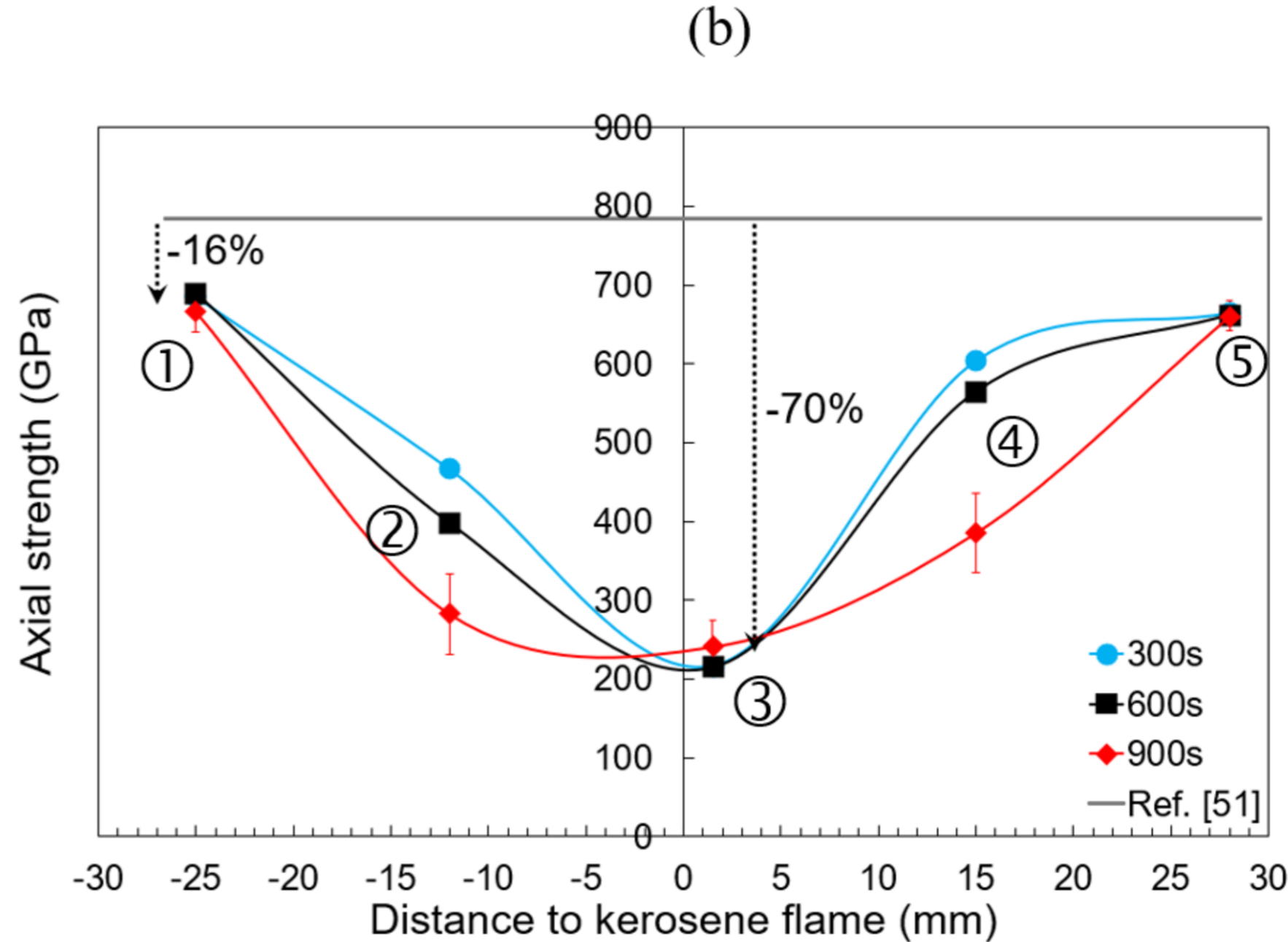
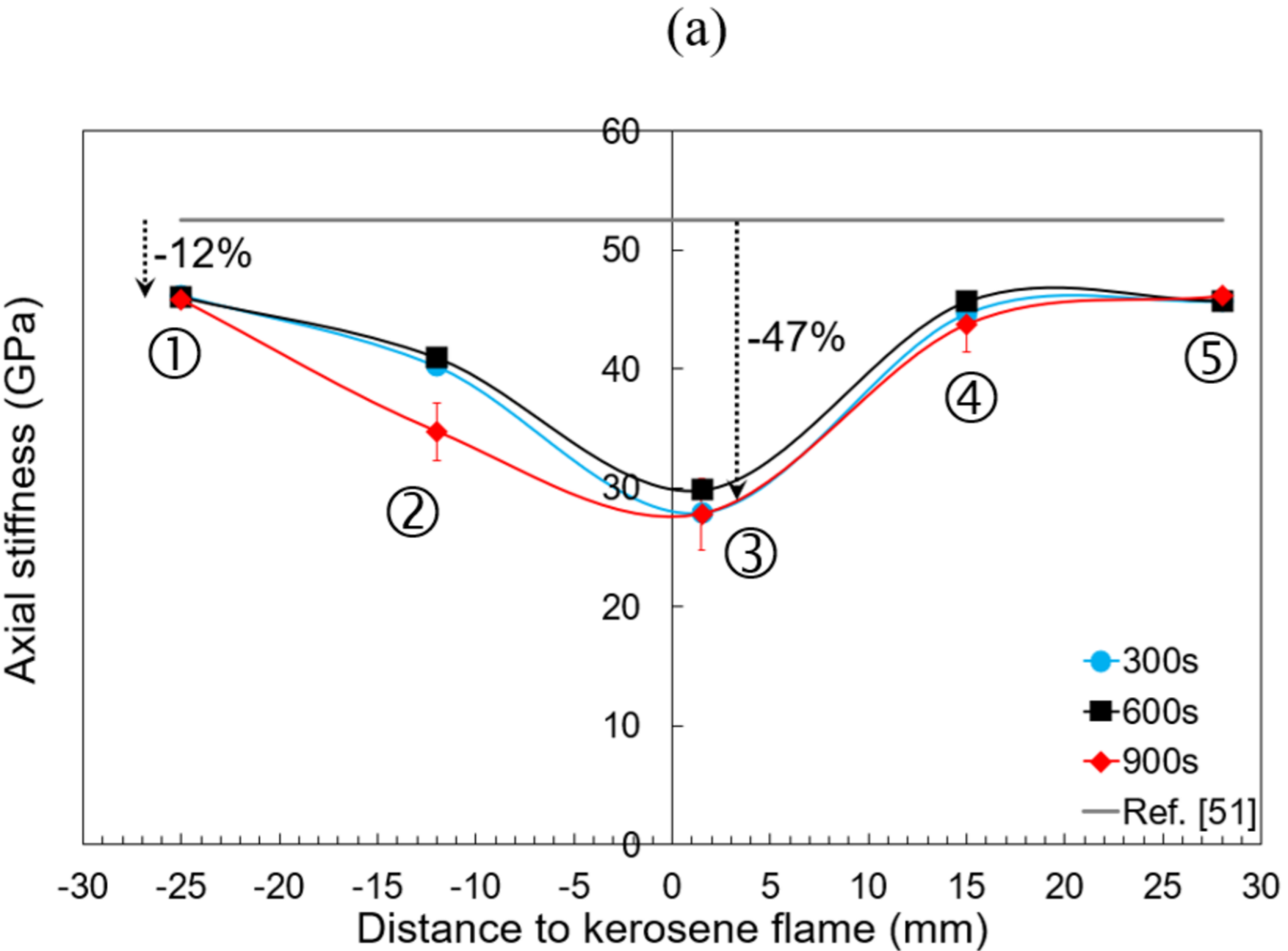


(b)



(c)

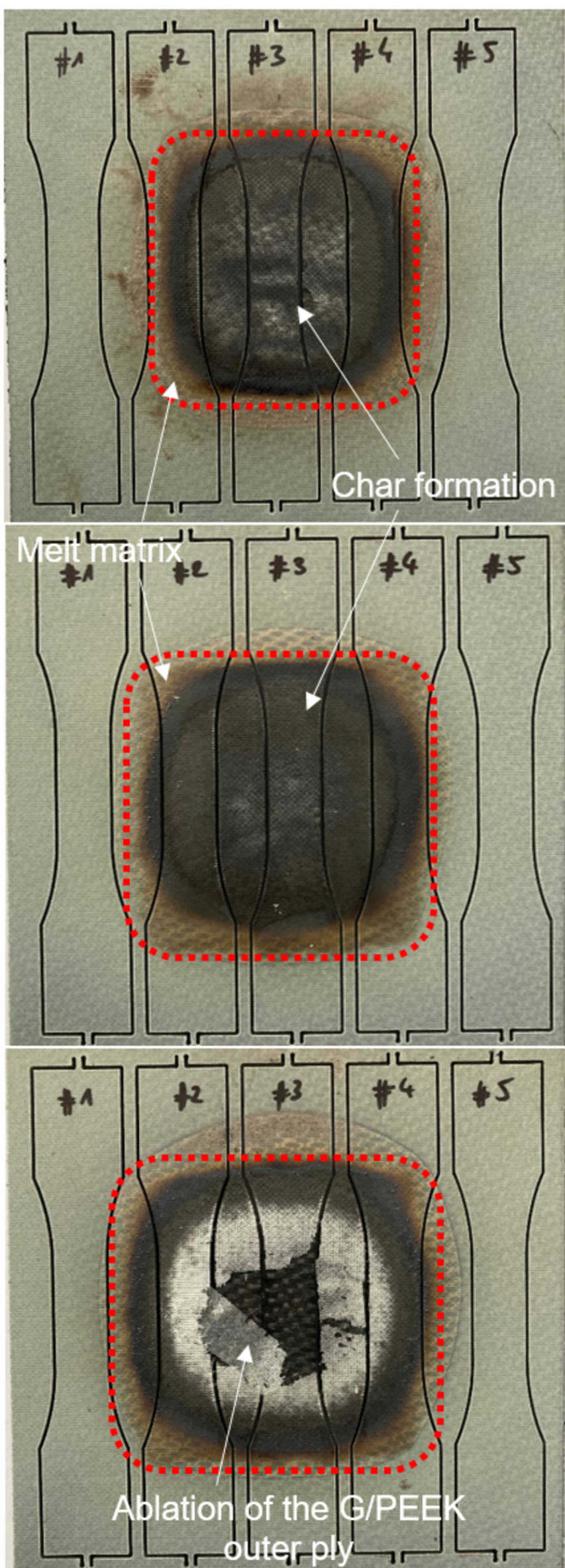




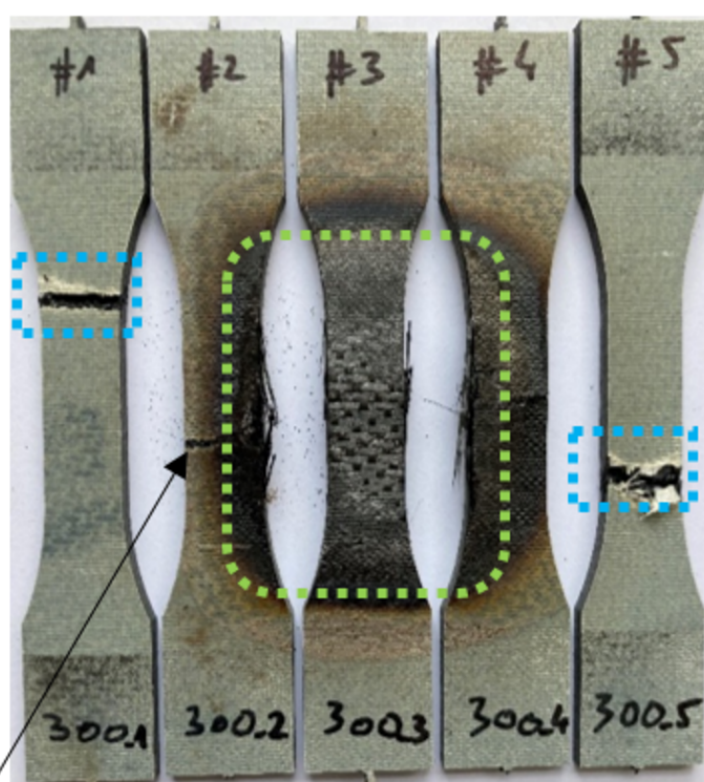


(a) After kerosene flame exposure

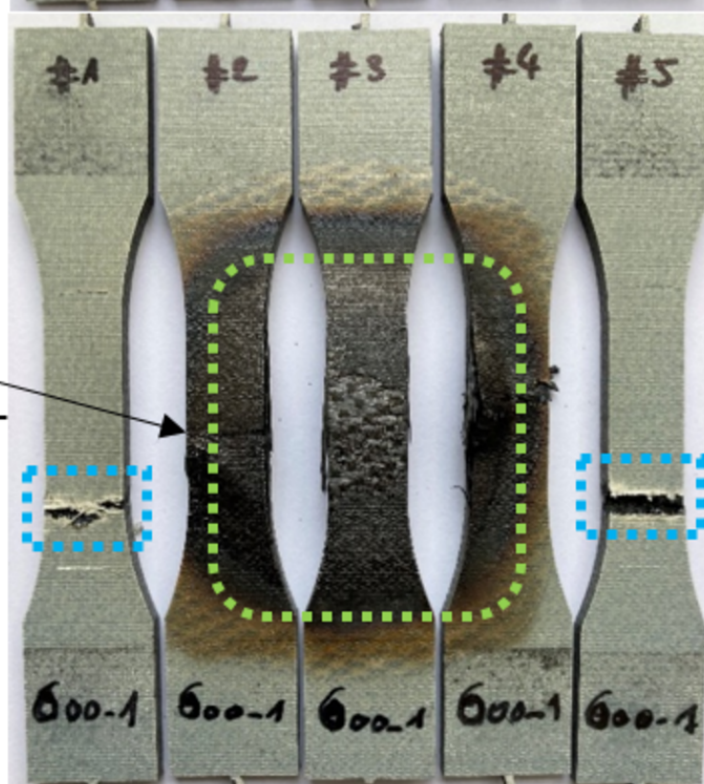
(b) After tensile testing



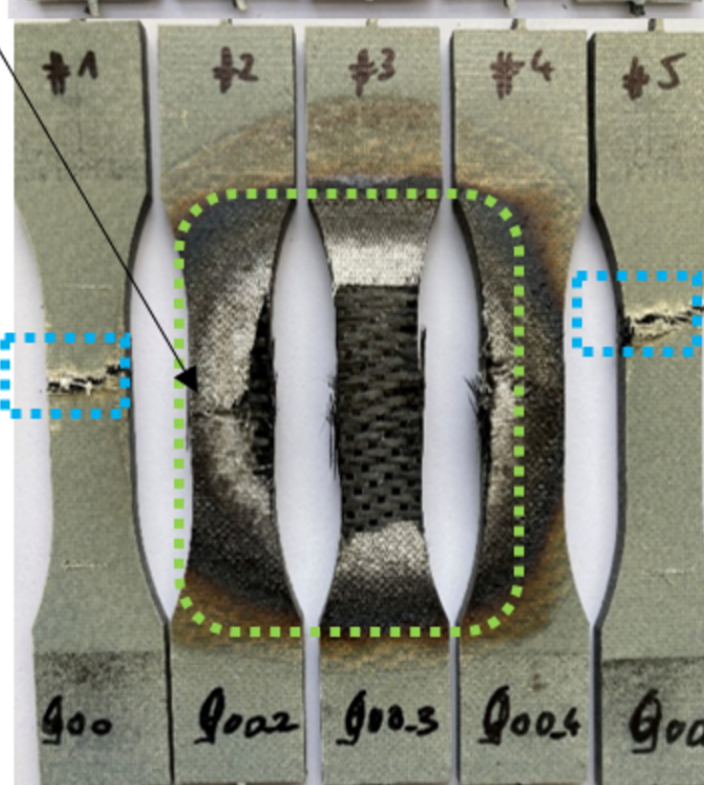
5 min




10 min





15 min



15 mm

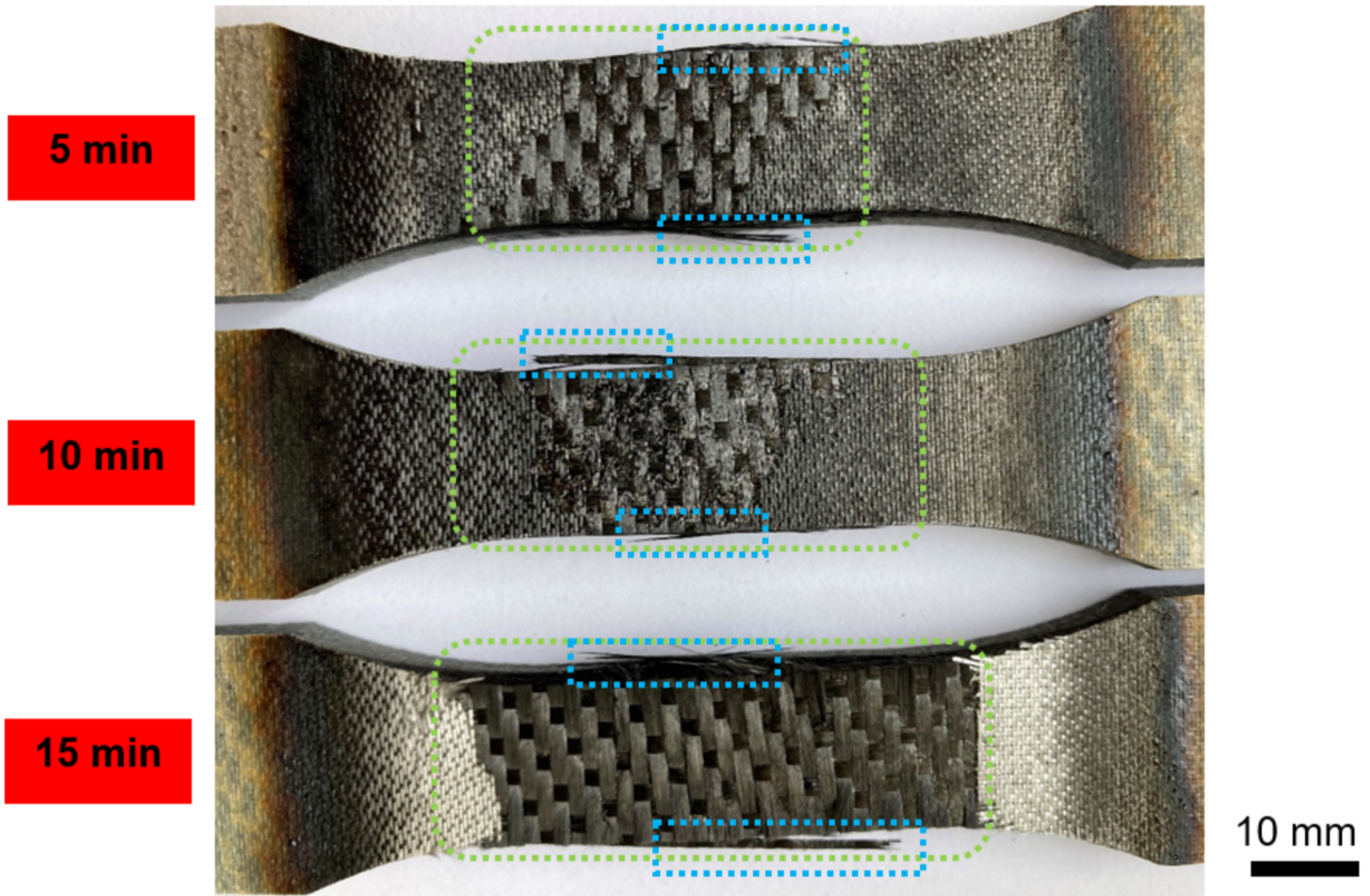
 Kerosene flame degraded area

 Brekage of 0° fibers

 Extensively delaminated area

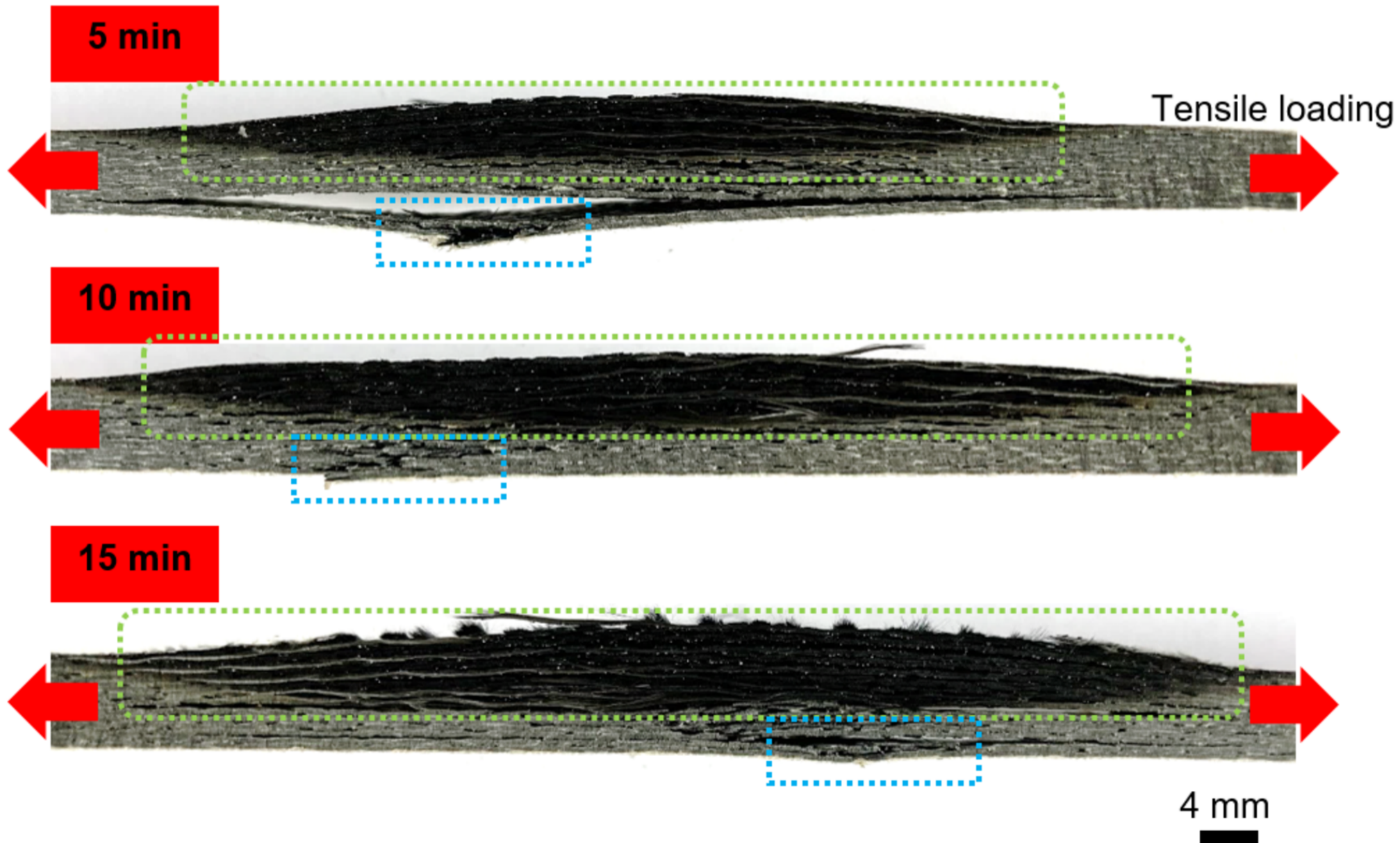


(a) Kerosene flame exposed surface (most degraded specimen in central position)



Extensively delaminated area Brekage of 0° fibers

(b) Macroscopic view of laminates' edges (most degraded specimen in central position)

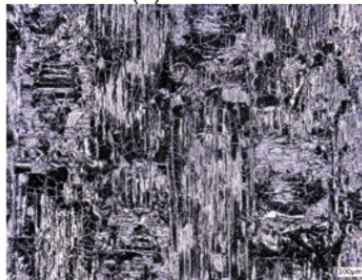




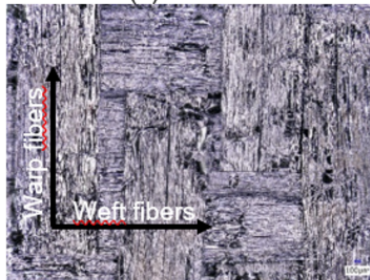
(a) 5 min

Exposed surface  
(b) 10 min

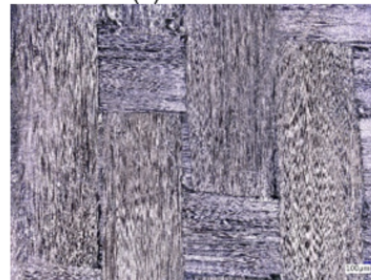
(c) 15 min



Char formation + melt PEEK matrix



Melt PEEK matrix + PEEK matrix pyrolysis



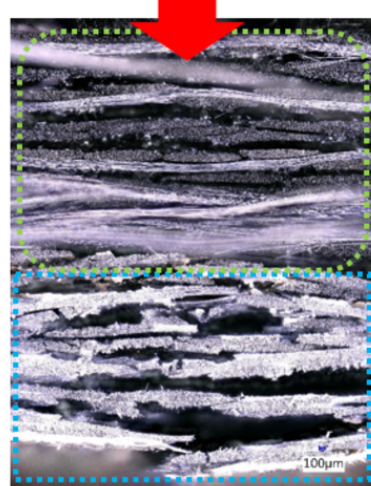
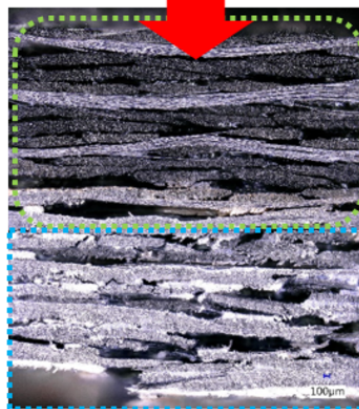
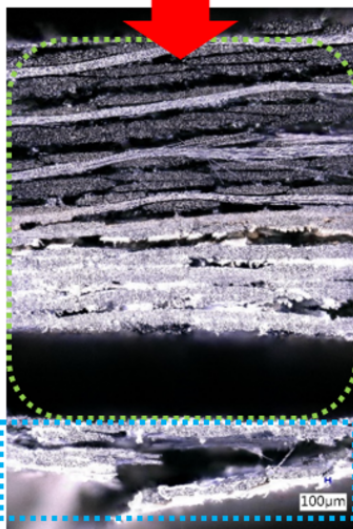
PEEK matrix pyrolysis + dry fibers network


Edge views

Kerosene flame

Kerosene flame

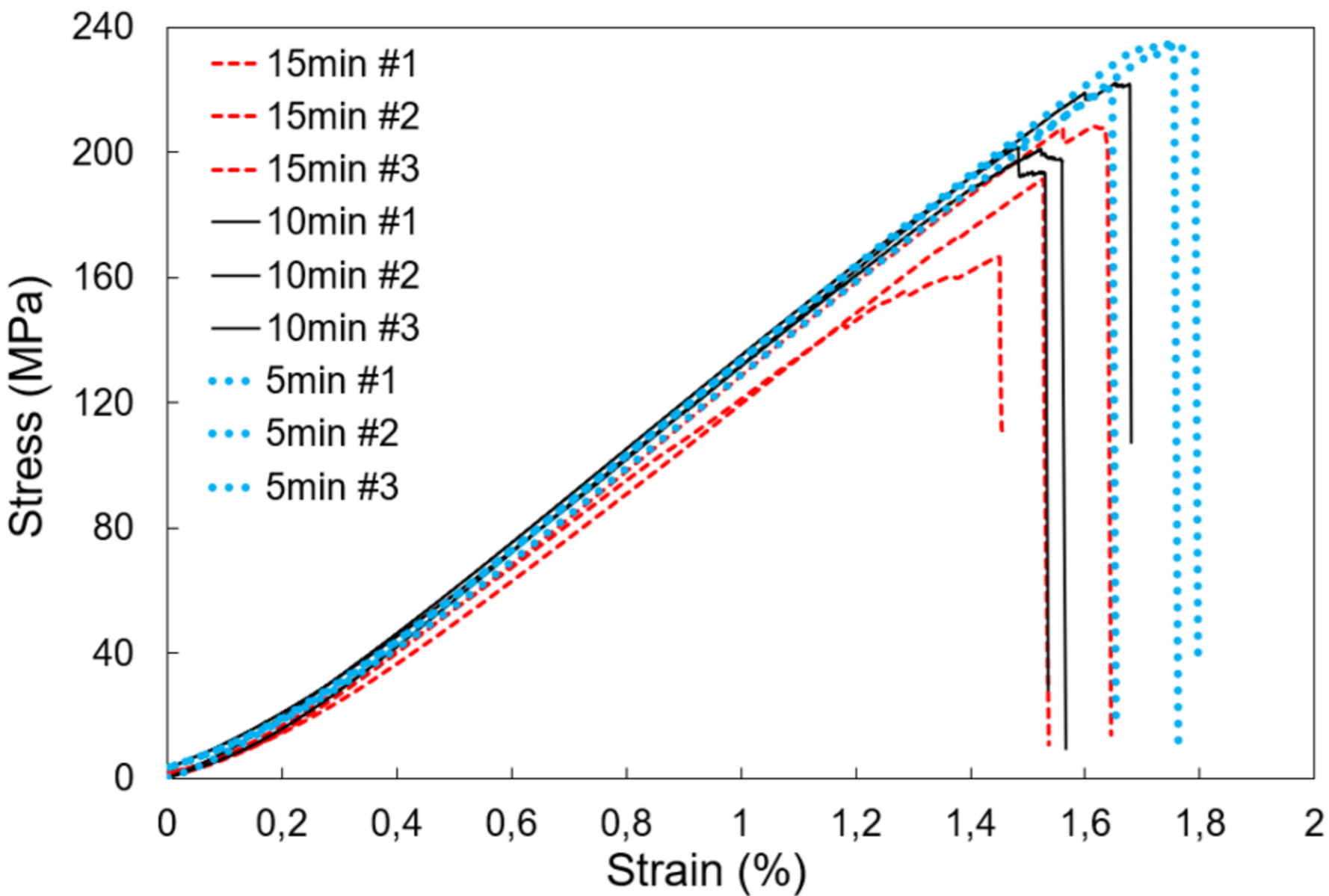
Kerosene flame



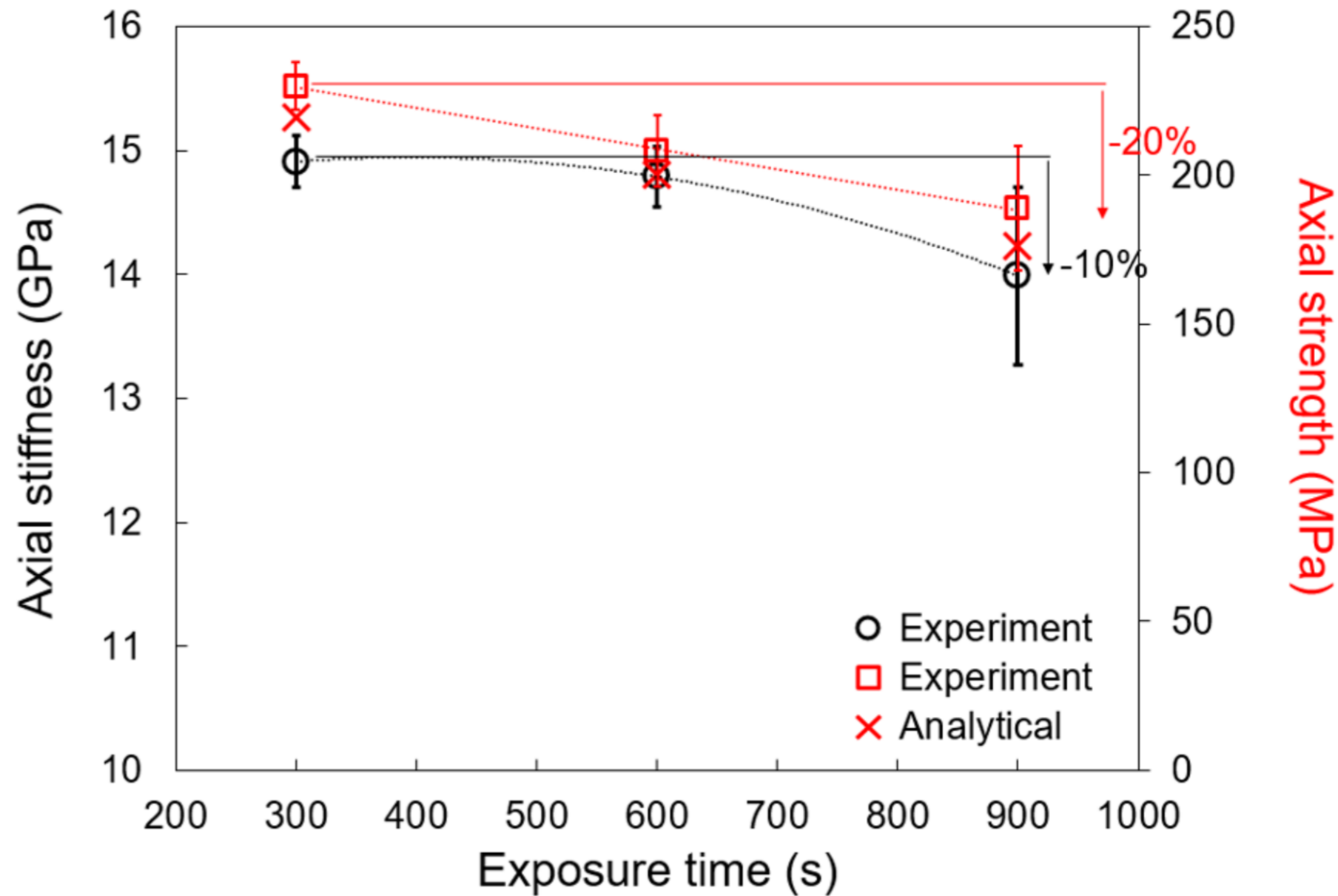
 Extensively delaminated area

 Brekage of 0° fibers

(a)



(b)



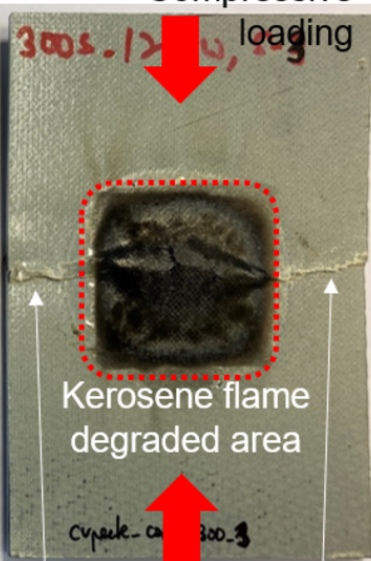


(a) 5 min

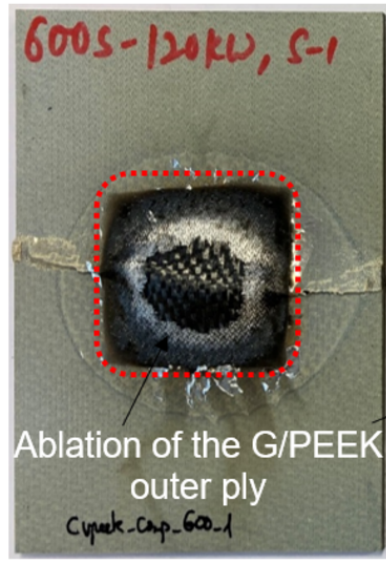
(b) 10 min

(c) 15 min

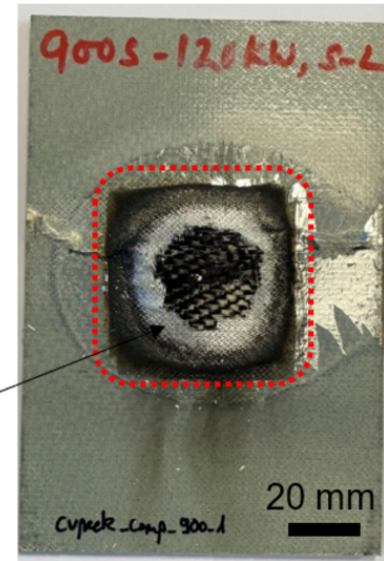
Compressive loading



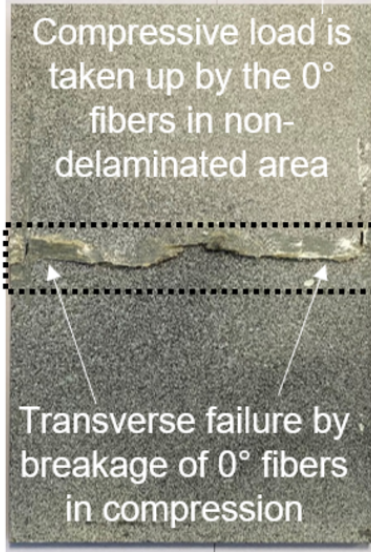
Kerosene flame degraded area



Ablation of the G/PEEK outer ply



20 mm



Compressive load is taken up by the 0° fibers in non-delaminated area

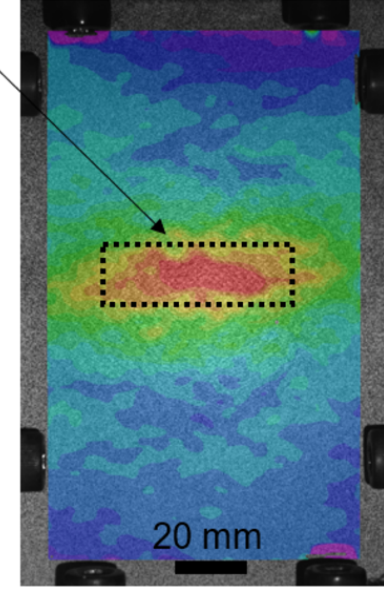
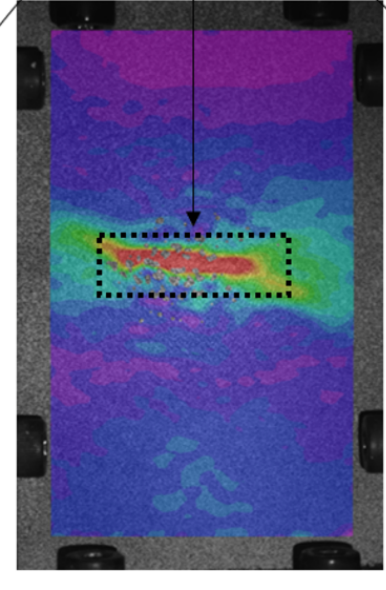
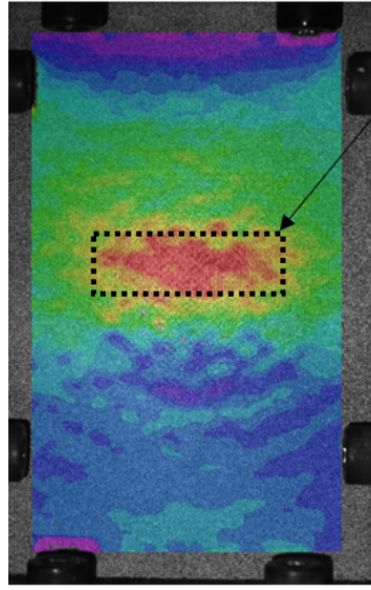
Transverse failure by breakage of 0° fibers in compression



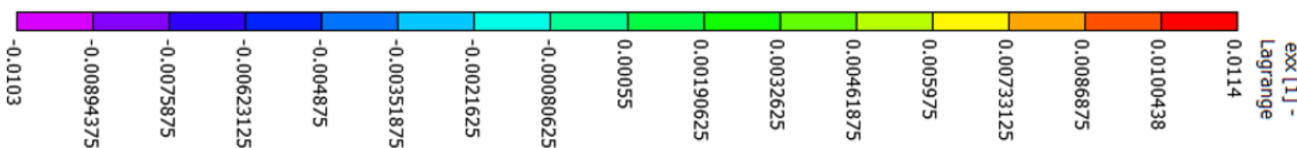
Formation of a plastic buckling band initiated in the delaminated area



20 mm



20 mm



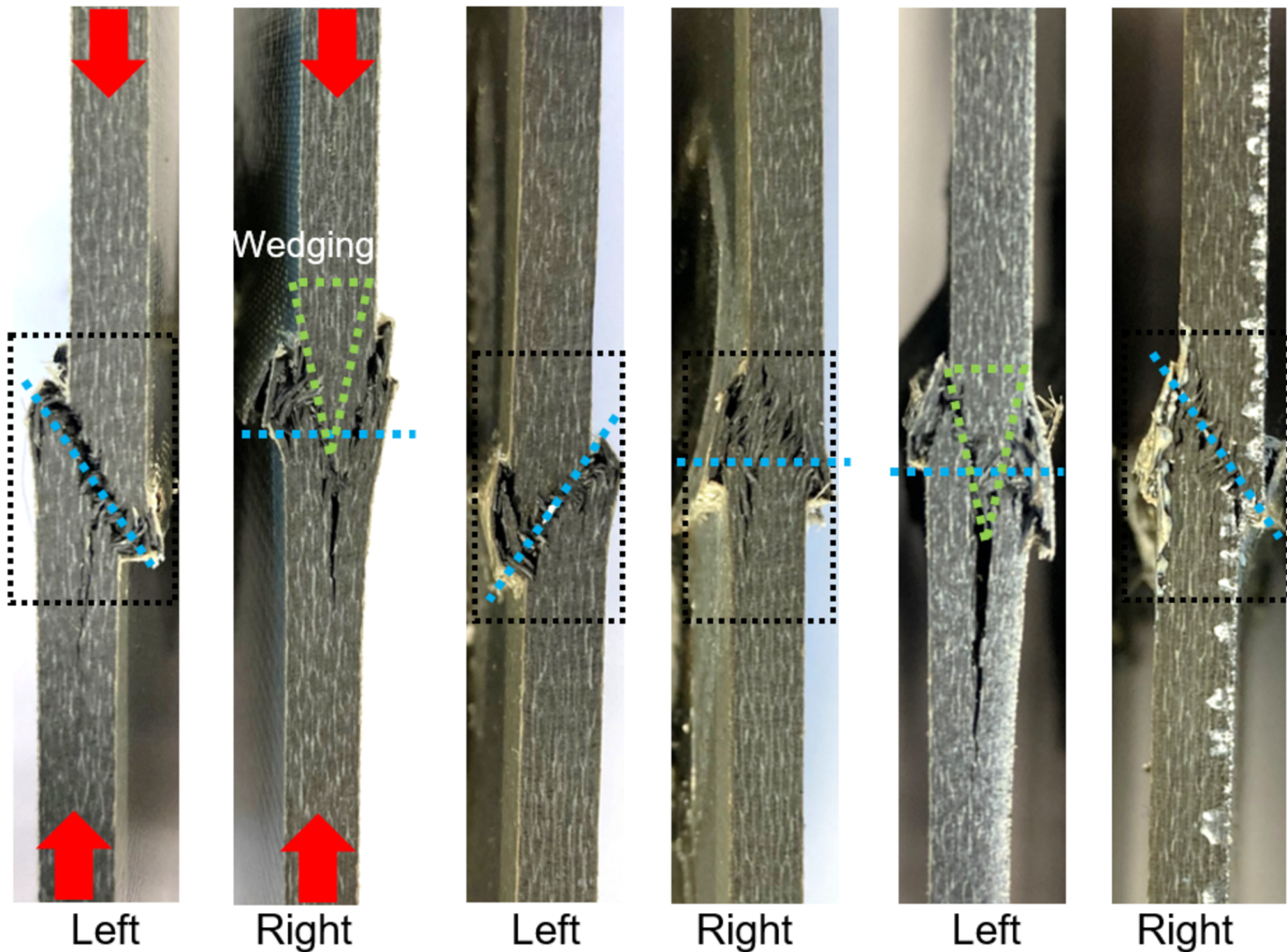
ex: [1] - Lagrange




(a) 5 min


(b) 10 min

(c) 15 min



Wedging

 Formation of a plastic buckling band initiated in the delaminated area

 Transverse failure by breakage of  $0^\circ$  fibers in compression